Progress in Oceanography 217 (2023) 103075

Contents lists available at ScienceDirect

Progress in Oceanography

journal homepage: www.elsevier.com/locate/pocean

Chemolithoautotrophic denitrification intensifies nitrogen loss in the Eastern Arabian Sea Shelf waters during sulphidic events

Anil Pratihary [a,b,*], Gaute Lavik [b], S.W.A. Naqvi [a,b,c], Gayatri Shirodkar [a], Amit Sarkar [a,d], Hannah Marchant [b,e], Thomas Ohde [f], Damodar Shenoy [a], Siby Kurian [a], Hema Uskaikar [a], Marcel M.M. Kuypers [b]

[a] Chemical Oceanography Division, CSIR-National Institute of Oceanography, Dona Paula, Goa 403 004, India
[b] Department of Biogeochemistry, Max-Planck-Institut für Marine Mikrobiologie, Celsiusstraße 1, D-28359 Bremen, Germany
[c] Department of Earth Sciences, Indian Institute of Technology, Kanpur, Uttar Pradesh 208016, India
[d] Environment and Life Sciences Research Centre, P.O. Box 1638, Kuwait Institute for Scientific Research, Salmiya 22017, Kuwait
[e] MARUM – Center for Marine Environmental Sciences, University of Bremen, 28359 Bremen, Germany
[f] Climate Center, Bavarian Environment Agency, Hans-Högn-Straße 12, D-95030 Hof, Germany

ARTICLE INFO

Keywords:
Anoxia
Sulphide
Denitrification
Nitrous oxide
Chemoautotrophy
Shelf
India

ABSTRACT

The Eastern Arabian Sea Shelf i.e. Western Indian Continental Shelf (WICS) – a known biogeochemical hotspot is characterized by monsoonal upwelling, seasonal O_2 deficiency, extremely high N_2O build-up and sulphidic events. The frequency and duration of the sulphidic events have increased over the last two decades, but their impact on the pelagic N cycling, N budget, and N_2O dynamics is poorly constrained. Thus, to address these problems and assess their implications on WICS biogeochemistry, we carried out physico-chemical measurements, ^{15}N-labeled incubations and bag incubations on five transects over the shelf during the sulphidic event (September-October) of 2011. We observed very high rates of sulphide-driven chemolithotrophic denitrification (1885–5825 nM N_2 d^{-1}) in the sulphidic, nitrate-depleted waters, and its potential occurrence in the sulphide-free, nitrate-replete waters (460–3137 nM N_2 d^{-1}), along with high transient N_2O production, and comparably low rates of anammox (0–119 nM N_2 d^{-1}) and DNRA (0–45 nM N d^{-1}). Despite the predominant cloud cover during the monsoon season, we could for the first time show the satellite image of a large colloidal sulphur (S^0) plume associated with the sulphidic event off Western India providing further evidence of extensive sulphide oxidation coupled to denitrification. Sulphide-driven denitrification (mean rate = 2697 nM N_2 d^{-1}) appeared to be the dominant N loss process during the anoxic regime (September-October) replacing the chemoorganotrophic (i.e. heterotrophic) denitrification (342 nM N_2 d^{-1}) that predominates during the preceding suboxic regime (July-August). Overall, the highest sulphide-driven denitrification rate over the WICS was found to be the second highest among the anoxic coastal systems of the world. Furthermore, simultaneous consumption of NO_x^- and S^{2-} at a ratio close to the theoretical value in the anaerobic incubations of chemocline waters indicated that the sulphide-driven denitrifiers were fixing carbon. The estimated dark C production (0.21 g C m^{-2} d^{-1}) due to chemolithoautotrophic denitrification was 18% of the photoautotrophic production and accounted for 15% of the total column productivity. Based on our conservative estimates, the chemolithoautotrophic denitrification was responsible for the removal of 0.4 Tg of fixed N and 0.57 Tg of sulphide, and fixation of 0.1 Tg of carbon annually in the shelf waters. Thus, the sulphidic event impacted the biogeochemistry and ecology, and modulated the N loss pathways and rates over the WICS. With the expansion and intensification of OMZs induced by global climate change, and the spreading of dead zones due to increasing anthropogenic activities, chemolithoautotrophic denitrification is likely to become increasingly significant in oceanic N cycle and impact the N budgets of shallow marine systems particularly.

* Corresponding author at: Chemical Oceanography Division, CSIR-National Institute of Oceanography, Dona Paula, Goa 403 004, India.
E-mail address: apratihary@nio.org (A. Pratihary).

https://doi.org/10.1016/j.pocean.2023.103075
Received 21 December 2022; Received in revised form 29 April 2023; Accepted 17 June 2023
Available online 21 June 2023

1. Introduction

Coastal sulphidic events are known to have deleterious impacts on pelagic and benthic life forms, their diversity and ecology, and modify the ecosystem functioning and biogeochemistry often irreversibly, resulting in serious socio-economic consequences and multiple challenges to ecosystem management worldwide (Diaz and Rosenberg, 2008; Breitburg et al., 2018). Anthropogenic activities and global climate change are causing the expansion and intensification of marine oxygen minimum zones (OMZs) (Stramma et al., 2008; Diaz and Rosenberg, 2008; Breitburg et al., 2018; Pitcher et al., 2021) more prominently in coastal oceans (Gilbert et al., 2010). Evidently, more than 500 coastal systems across the world have turned hypoxic ($O_2 < 62$ μM) since mid-20th century owing to the above stressors (Diaz and Rosenberg, 2008). However, the biogeochemical, ecological and climatic impacts of such deoxygenation are understudied in many coastal and shelf systems.

The bioavailability of fixed inorganic N predominantly controls oceanic primary production (Falkowski, 1997; Tyrrell, 1999), and up to 50% of oceanic N-loss occurs in the four major OMZs i.e. the Arabian Sea, Eastern Tropical North Pacific (ETNP), Eastern Tropical South Pacific (ETSP) and Eastern Tropical South Atlantic (ETSA) (Codispoti et al., 2001) via microbially mediated processes such as heterotrophic denitrification (Ward et al., 2008; Dalsgaard et al., 2012) and anaerobic ammonium oxidation i.e. anammox (Hamersley et al., 2007; Kuypers et al., 2005; Thamdrup et al., 2006). In addition, N-transformation processes such as dissimilatory NO_x^- (NO_3^- and/or NO_2^-) reduction to NH_4^+ (DNRA) as well as microaerobic nitrification (NH_4^+ and NO_2^- oxidation) have been shown to be important to N-cycling in some OMZs (Kartal et al., 2007; Lam et al., 2009; Füssel et al., 2012; Bristow et al., 2016).

Apart from the open ocean OMZs, there are numerous seasonal or perennial hypoxic/anoxic coastal and shelf systems, and semi-enclosed basins (Pitcher et al., 2021) which are also significant hotspots of N loss; most notably the Black Sea (Kuypers et al. 2003; Fuchsman et al., 2012), Baltic Sea (Brettar and Rheinheimer, 1991; Bonaglia et al., 2016), Cariaco Basin (Montes et al., 2013; Suter et al., 2021), Gulfo Dulce Bay (Dalsgaard et al., 2003), Saanich Inlet (Manning et al. 2010; Michiels et al., 2019), Mariager Fjord (Jensen et al., 2009), Namibian Shelf (Kuypers et al, 2005; Lavik et al., 2009), Peruvian Shelf (Schunck et al., 2013) and Chilean Shelf (Galán et al., 2014). Many of these shallow systems turn sulphidic due to benthic flux of sulphide (defined as $H_2S + HS^- + S^{2}$). Consequently, at the pelagic NO_x^--H_2S chemocline, microorganisms can couple denitrification to sulphide oxidation (Eq. (1) or (2)). These microorganisms oxidize sulphide to either elemental sulphur or sulphate and are often autotrophs i.e. they fix inorganic carbon (Schunck et al., 2013; Callbeck et al., 2021). There is extensive evidence that denitrifying, sulphide-oxidizing autotrophs belonging to γ- and Ɛ-proteobacteria and particularly the SUP05 clade (Walsh et al., 2009) are abundant and active in the sulphidic waters and redoxclines of OMZs worldwide (Campbell et al., 2006; Canfield et al., 2010; Glaubitz et al., 2013; Callbeck et al., 2018; van Vliet et al., 2020), although other species such as *Thiomicrospira* spp., *Sulfurimonas* spp., *Candidatus* spp. *and Arcobacter* spp. are also commonly reported in some anoxic coastal systems (Brettar et al., 2006; Glaubitz et al., 2009, 2010; Lavik et al., 2009; Grote et al., 2012; Michiels et al., 2019).

$$8NO_3^- + 5HS^- + 3H^+ \rightarrow 5SO_4^{2-} + 4N_2 + 4H_2O \quad (1)$$

or

$$2NO_3^- + 5HS^- + 7H^+ \rightarrow 5S^0 + N_2 + 6H_2O \quad (2)$$

(Burgin and Hamilton, 2008; Lam and Kuypers, 2011)

Chemolithoautotrophic denitrification impacts the biogeochemistry and ecology of coastal and shelf systems in multiple ways. For instance, it reportedly removes up to 70% of extraneous N in the Baltic Sea thereby reducing the possible occurrence of eutrophication (Dalsgaard et al., 2013), furthermore the process is associated with substantial dark CO_2 fixation (Taylor et al., 2001; Hügler et al., 2005; Jost et al., 2008). By removing H_2S, chemolithotrophic denitrifiers effectively detoxify the water column as sulphide is highly toxic to marine organisms (Levin et al., 2009; Vaquer-Sunyer and Duarte, 2010; Lavik et al., 2009). Sulphide-driven denitrification also has the potential to impact the emissions of N_2O, a potent green house and ozone depleting gas. Intriguingly, even though many coastal anoxic ecosystems are significant N_2O sources, N_2O remains generally undetectable or undersaturated in their sulphidic bottom waters (Brettar and Rheinheimer, 1991; Naqvi et al., 2010; Schunck et al., 2013; Arévalo-Martínez et al., 2015, 2019). Thus, from biogeochemical, ecological and climatic perspectives, chemolithoautotrophic denitrification has important implications that necessitate comprehensive investigation. With the increasing number of coastal dead zones and frequency of anoxic events on global scale (Diaz and Rosenberg, 2008; Breitburg et al., 2018), it is imperative to understand how their N biogeochemical cycles are likely to respond to such changes.

Western Indian Continental Shelf (WICS), the largest seasonal coastal anoxic system and a biogeochemical hotspot, is one such system which has remarkably transformed from being suboxic (defined throughout as $O_2 \leq 4.4$ μM, $NO_x^- > 0$ μM and $H_2S = 0$ μM (Naqvi et al., 2010)) to anoxic (defined throughout as $O_2 = 0$ μM, $NO_x^- = 0$ μM and $H_2S > 0$ μM, or sulphidic/euxinic (Naqvi et al., 2010)). The duration and frequency of the sulphidic events on the WICS have been increasing over last couple of decades due to natural causes and/or increasing anthropogenic activities (i.e. nutrient loading through terrestrial run-off and atmospheric deposition) over the Indian subcontinent (Naqvi et al., 2006, 2009; Gupta et al., 2021). Oxygen deficiency over the shelf sets in with the advent of the southwest monsoon-induced upwelling in June and intensifies over time, exacerbated by strong thermohaline stratification. During the late southwest monsoon (September-October), the water column becomes NO_x^--depleted, and the bottom waters turn sulphidic, mostly due to sulphide release from the sediments (Pratihary et al., 2014) as documented in similar systems elsewhere (Lavik et al., 2009; Schunck et al., 2013; Galán et al., 2014). Euxinia prevails in the bottom waters until October after which the surface currents reverse and normoxia is re-established. The WICS is probably the only coastal system in the world wherein hypoxic, suboxic and anoxic redox regimes co-occur over outer-shelf, mid-shelf and inner-shelf of the same segment, respectively with such regularity.

The seasonal occurrence of sulphidic events over the WICS was observed as early as 1997 (Naqvi et al. 2000), and since then, NIO's time series observation (CaTS) has shown the frequent occurrence of sulphidic event over the WICS during September to October (Naqvi et al., 2006, 2009). Its increasing frequency is evident from the occurrence of 6 sulphidic events within a decade (1997–2007; Naqvi et al., 2009). Conservative estimates derived from Naqvi et al. (2000) and Shirodkar et al. (2018) show that the area affected by sulphidic event extends from off Kochi (9°N) in the south to off Mumbai (18°N) in the north, and is restricted to up to a mean depth of 35 m over the innershelf thereby occupying an area of ~ 16,000 Km^2 which is ~ 9% of the area of the entire hypoxic zone (i.e. 180,000 Km^2) over the WICS. However, the extremity, areal extent and duration of the sulphidic event vary over spatial and annual scales largely due to annual oscillation of the Indian Ocean Dipole (IOD) (Parvathi et al., 2017). For instance, in a few extreme cases (e.g. year 1998, 1999, 2001 and 2003), the sulphidic event lasted from mid-August to October, and the sulphidic zone extended up to the mid-shelf (depth > 50 m) with H_2S reaching up to 19 μM, 14 μM, 15 μM and 26 μM H_2S off Mumbai, Goa, Mangalore, and Kochi, respectively (Naqvi et al., 2000, 2009; Shirodkar et al., 2018). However, the impact of sulphidic events on the pelagic biogeochemistry, and in particular N-cycling has remained poorly understood.

Massive N loss has been reported over the WICS during Southwest monsoon season based on δ^{15}N-NO_3^- and δ^{18}O-NO_3^- measurements and

^{15}N-incubation studies (Naqvi et al., 2006; Bardhan and Naqvi, 2020; Sarkar et al., 2020). Hitherto, denitrification has been reported to be largely the dominant N loss process with anammox and DNRA being mostly insignificant (Sarkar et al., 2020). Interestingly, Sarkar et al. (2020) observed that (1) the mean denitrification rate during a sulphidic event (i.e. year 2009) was > 2 fold higher than during non-sulphidic events (i.e. years 2008, 2010), and (2) anammox rates were below detection during the sulphidic event, but were relatively higher during the non-sulphidic conditions. Their study indicated that sulphidic event inhibits anammox and intensifies denitrification in the shelf waters. Furthermore, Naqvi et al. (2006, 2009) observed extremely high N_2O build-up (~0.8 μM) at the oxic-anoxic interface of the shelf water column only during suboxia-anoxia transition period (early September) i.e. when sulphide just starts to build up, which implies that such high N_2O build-up is someway related to the sulphidic events. As the oxygen deficiency over the WICS has intensified over the last 4 decades leading to extended periods of anoxia (Naqvi et al., 2006, 2009), this can have important implications for the N cycling and budget over the shelf which

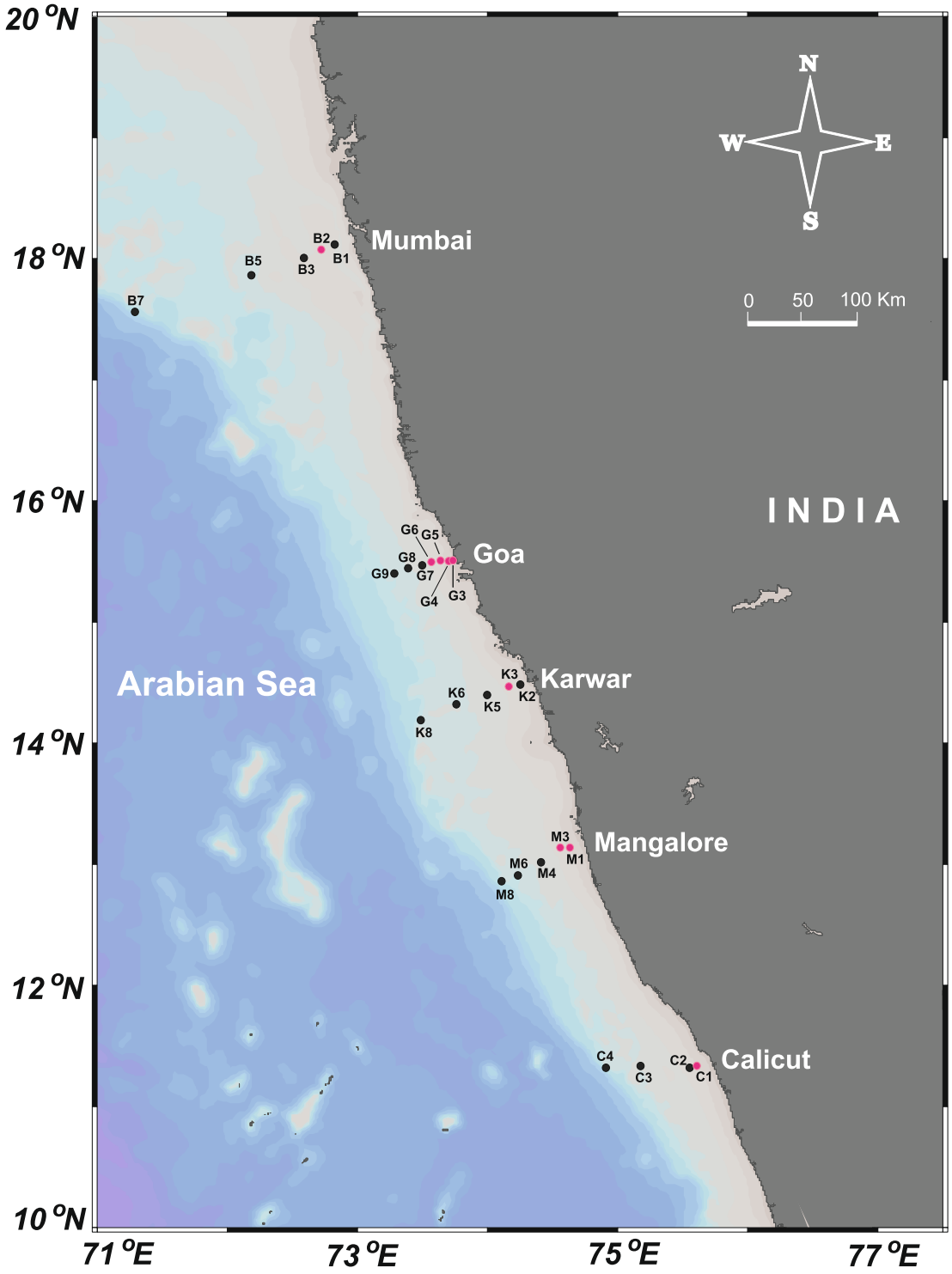

Fig. 1. Map of the study area. Dots denote the stations sampled for physical and biogeochemical parameters, and red dots denote the stations where ^{15}N-incubations were carried out.

necessitates a precise mechanistic understanding. We carried out a comprehensive study to understand the coupling of sulphur and nitrogen cycling, and its impact on pathways and rates of N loss through biogeochemical measurements, shipboard ^{15}N-labeled incubations and bag incubations at some selected stations (which were suboxic or anoxic) at five transects over the WICS during late SW monsoon. We hypothesize that sulphide-driven (chemolithoautotrophic) denitrification becomes the dominant process during late summer monsoon replacing heterotrophic denitrification, intensifies the N loss, and plays a key role in N_2O cycling in the WICS waters.

2. Materials and methods

2.1. Study area

Our study area is located over the inner continental shelf of Western India (Fig. 1). The WICS occupies an area of 310,000 km^2, of which the inner shelf comprises ~33% (Mallik, 2008). This region is strongly affected by the monsoons, i.e. the biannual reversal of winds and surface currents. Southwest monsoon causes moderate upwelling along the coast during June-September. Due to a unique interplay of physical, hydrographical and biogeochemical changes induced by the southwest monsoon (Naqvi et al., 2006; Parvathi et al., 2017), hypoxia develops over the outershelf and gradually covers the shelf segment between 11° to 18° N (Gupta et al., 2021). Upwelling brings NO_3^--rich (>20 μM) hypoxic water (O_2 < 20 μM) over the shelf which occupies an area of 180,000 Km^2 of the shelf area by September (Naqvi et al., 2006). Oxygen progressively falls to < 4 μM during July-August in the subsurface waters triggering denitrification which exhausts NO_3^- and NO_2^- by mid-September, and the system starts becoming sulphate-reducing (Naqvi et al., 2006; Sarkar et al., 2020). During peak suboxia, (July-August), the water column remains stratified with a 5–10 m thick low saline oxic surface layer overlying a high saline, NO_x^-- rich suboxic layer wherein NO_2^- (up to 8 μM) and N_2O (200–550 nM) accumulate. As the system transitions from suboxia to anoxia during early September, high N_2O accumulation (up to 765 nM) is often observed at suboxic-anoxic/oxic-anoxic interface (Naqvi et al., 2000). During September to October, O_2 and NO_x^- fall below detection and the subsurface waters turn sulphidic, and become enriched in NH_4^+ and PO_4^{3-}. The intensity of the O_2 deficiency varies spatially along the shelf (north–south) and across the shelf (east–west) at a given time (Naqvi et al., 2006; Gupta et al., 2021), and is also modulated by phase change in IOD (Parvathi et al., 2017). Upwelling starts at off Kerala coast during June and progresses northward, and consequently a time lag of ~ 2 weeks in the development of anoxia has been observed between the southern (off Kerala) and northern (off Goa) part of the shelf. Anoxia at southern transects (off Kerala and Mangalore) is often found to be more intense compared to northern transects (off Mumbai, Goa and Karwar) during September-October. The WICS is the largest natural and seasonal hypoxic coastal system of the world wherein all three types of redox regimes co-occur across and along the shelf. During November–February, the prevailing northeast monsoon-induced West India Coastal Current (WICC) causes downwelling which reinstates the normoxia that continues till May.

2.2. Physical and biogeochemical sample collection

We covered 5 transects over the WICS (Fig. 1) to carry out our study i.e. off Mumbai (18ºN), off Goa (15ºN), off Karwar (14ºN), off Mangalore (13ºN) and off Calicut (11ºN) from 15th September to 7th October 2011 onboard *RV Sindhu Sankalp* (SSK024 cruise). Vertical profiles of temperature, salinity and potential density (σ_θ) were obtained from a CTD-Rosette sampler (Seabird Electronics). Samples for dissolved O_2, H_2S, N_2O and nutrients (NO_3^-, NO_2^-, NH_4^+, PO_4^{3-}) were collected at discrete depths using a CTD Rosette sampler at several stations along these transects. Dissolved O_2 samples were quickly fixed by adding 1 ml each of Winkler's solutions, and the oxyhydroxide precipitates were let to settle (Grasshoff et al., 1999). H_2S samples were fixed by addition of a mixed reagent of N, N-dimethyl-*p*-phenylenediamine dihydrochloride and $FeCl_3$ (Grasshoff et al., 1999). N_2O samples were immediately poisoned by adding saturated $HgCl_2$ solution (Naqvi and Noronha, 1991), and nutrient samples were kept at 4 °C in the dark until analysis (Grasshoff et al., 1999).

2.3. Satellite imaging of the sulphur plume

The sulphur plumes in the surface water layer were identified in MERIS (Medium Resolution Imaging Spectrometer) and MODIS (Moderate Resolution Imaging Spectroradiometer) images in the expedition period of 15 September to 7 October 2011 as per the methodology of Ohde and Dadou (2018). The corresponding satellite scenes were searched for sulphur events in the study area between Mumbai (18° N) and Calicut (11ºN). The method for the identification of sulphur plumes was based on the different optical properties of different water masses in the study area. The sulphur plumes can be clearly distinguished by their special spectral signatures (Suppl. Fig. 1) and milky turquoise color (Fig. 2). They are characterized by very high reflectances in all MERIS bands, especially at the green band of 559.7 nm. The spectral peaks of unaffected offshore and onshore waters, and river plumes are in the blue or green wavelength range depending on the composition of optically active water constituents like chlorophyll-*a*, yellow substances and suspended matter. The offshore waters with low chlorophyll-*a* concentration are characterized by maxima in the MERIS channel of 489.9 nm. The spectra of the onshore waters are influenced by the absorption of chlorophyll-*a* at MERIS bands of 442.6 nm and 664.6 nm. The river plumes with higher concentrations of yellow substances and suspended matter are qualified by their higher spectral peaks compared to the offshore and onshore waters. The river plumes are differentiated from sulphur plumes by their different spectral slopes in the red wavelength range.

2.4. Shipboard ^{15}N-labeled incubations

We carried out a series of shipboard ^{15}N-labeled incubations at stations B2 (off Mumbai), G3, G4, G5 and G6 (off Goa), K3 (off Karwar), M1 and M3 (off Mangalore) and C1 (off Calicut) onboard R/V *Sindhu Sankalp* during September-October 2011 following the methodology by Holtappels et al. (2011). Water samples from selected suboxic/anoxic depths were collected in five 250 ml serum bottles with extreme precaution to avoid O_2 contamination. Thereafter, the waters were purged with zero-grade helium (Praxair; 99.999%) for 15 min to lower the background $^{28}N_2$ level, and then spiked with substrates i.e. 8 μM $^{15}NO_2^-$, 8 μM $^{15}NO_2^-$ + 5 μM Na_2S, 8 μM $^{15}NO_2^-$ + 10 μM Na_2S, 8 μM $^{15}NO_2^-$ + 15 μM Na_2S and 8 μM $^{15}NH_4^+$. The loss of native sulphide due to He purging has been shown to be negligible (~2.5%) (Dalsgaard et al., 2013) as ~ 97% of the total sulphide pool in seawater remains in the form of HS^- (Millero, 1986). The concentrations of the above substrates were chosen so as to mimic their natural concentrations in the WICS waters during seasonal anoxia wherein NO_2^- and NH_4^+ build up to average of ~8 μM each and H_2S builds up to an average of ~5 μM, respectively (Naqvi et al., 2000, 2006, 2009). However, since H_2S level can reach up to ~ 15 μM or higher during extreme anoxic events (Naqvi et al., 2000; Shirodkar et al., 2018), varying concentrations of S^{2-} (i.e. 5, 10 and 15 μM) were added along with $^{15}NO_2^-$ in order to understand the impact of increasing sulphide level on N_2O and N_2 production. ^{15}N substrates were also purged with helium prior to the addition. Details of substrate combination are presented in Table 1. The Na_2S standard solution (50 mM) was prepared in helium-purged deionized water inside an N_2-flushed anoxic chamber. Spiked samples in each bottle were transferred to five 12 ml exetainer vials (Labco Ltd., UK) after sufficient flushing, and the vials were quickly capped without any head-space. Then the vials were stored in the dark and at temperature close to the in-situ temperature for 48 h. The sampling time points were taken at/close to

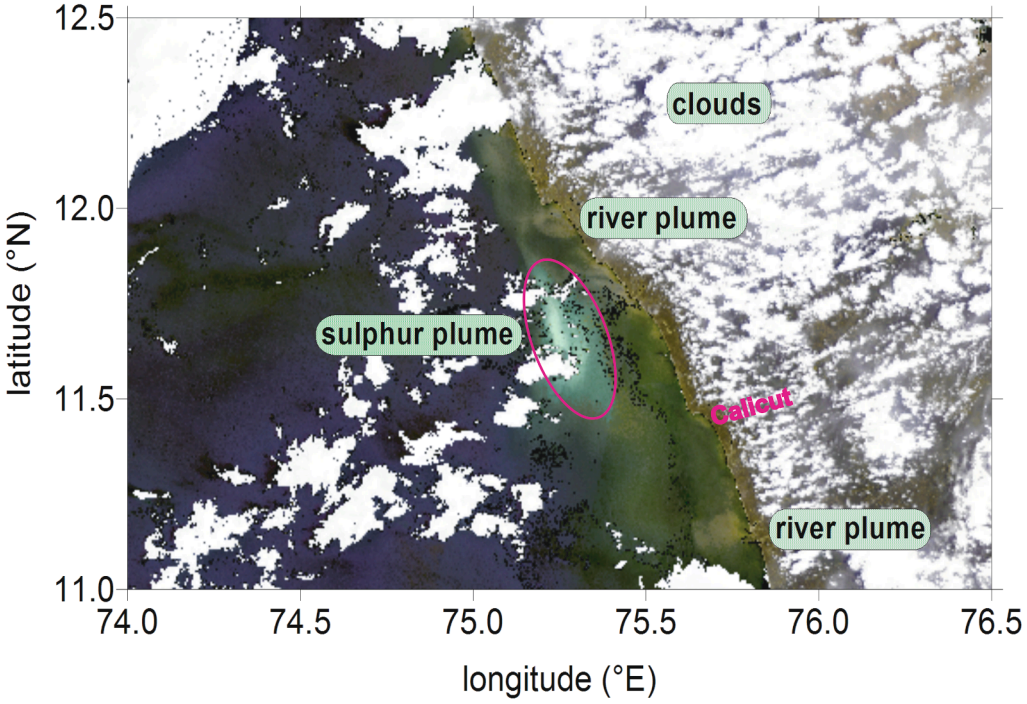

Fig. 2. Satellite-derived image of sulphur plumes (encircled milky turquoise patch) in WICS waters.

Table 1
Details of ^{15}N-labeled incubations. √ indicates that the incubation with the specified substrate was carried out at that particular depth/station.

Station	Depth (m)	Substrates added in ^{15}N-labeled incubation				
		8 μM $^{15}NO_2^-$	8 μM $^{15}NO_2^-$ +5μM Na_2S	8 μM $^{15}NO_2^-$ +10 μM Na_2S	8 μM $^{15}NO_2^-$ +15 μM Na_2S	8 μM $^{15}NH_4^+$
B2	34	√	√	√	√	√
G3	6	√	√	√	√	√
	13	√	√	√	√	√
G4	7	√	√	√	√	√
	15	√	√	√	√	√
G5	14	√	√	√	√	√
	20	√	√	√	√	√
	25	√	√	√	√	√
G6	28	√	√	√	√	√
	34	√	√	√	√	√
K3	20	√	√	√	√	√
	30	√	√	√	√	√
M1	15	√	√	√	√	√
M3	25	√	√	√	√	√
C1	7	√	√	√	√	√
	15	√	√	√	√	√

0, 12, 24, 36 and 48 h by introducing 2 ml of helium into the vials followed by addition of 100 μL of saturated $HgCl_2$ solution. After mixing vigorously, the vials were kept inverted until analysis in order to minimize the exchange of headspace gas with atmosphere through the septum.

2.5. Incubation of the chemocline waters

A set of bag incubations of water from just below the chemocline (oxic-suboxic or oxic-anoxic interface) depth at a suboxic station (G6) and anoxic station (G5) was also carried out in order to further confirm the coupling of NO_x^- reduction to sulphide oxidation (See Table 2). At G6, water from 28 m (0 μM NO_3^-, 0.29 μM NO_2^-, 0 μM H_2S) was collected into two 1.5 L Trilaminate gas-tight bags (Pollution measurement corporation, USA). At G5, water from 14 m depth (0 μM NO_3^-, 0.27 μM NO_2^-, 0 μM H_2S) was collected into six 1.5 L Trilaminate gas-tight bags. All the bags were flushed with helium, and evacuated prior to the filling of water samples. After sampling, the small helium headspaces were quickly removed from the bags and the bags were kept at close to in-situ temperature. One bag each from G6 (Bag-A) and G5 (Bag-C) were enriched with 8 μM of $^{14}NO_2^-$ and one other bag each from G6 (Bag-B) and G5 (Bag-D) were spiked with 8 μM of $^{14}NO_2^-$ and 5 μM Na_2S. The bags were incubated at in-situ temperature for 48 h. No immediate treatment was given to the remaining four bags (Bag E, F, G and H) collected at G5, and they were pre-incubated at temperature close to the in-situ temperature in order to allow the waters to turn sulphidic over time. After ~ 2 weeks of pre-incubation, the enclosed waters were observed to be sulphidic (~15 μM H_2S) and depleted in NO_x^- (NO_3^-, NO_2^-=0μM). Then the two bags (Bag-E and Bag-F) were spiked with 16 μM $^{14}NO_3^-$ and the other two bags (Bag-G and Bag-H) were enriched with 8 μM $^{14}NO_2^-$, and all the four bags were incubated at in-situ temperature

Table 2
Details of the bag experiments done at G6 and G5, Off Goa. * indicates that the substrate was not added but allowed to build up over time through pre-incubation.

Bag	Station, Depth	Substrates added	NO_x^- consumption rate (μmol L^{-1} h^{-1})	S^{2-} consumption rate (μmol L^{-1} h^{-1})	NO_x^- reduction: S^{2-} oxidation
A	G6, 28 m	8 μM NO_2^-	0.26	–	
B	G6, 28 m	8 μM NO_2^- + 5 μM S^{2-}	0.34	0.19	1.78
C	G5, 14 m	8 μM NO_2^-	0.11	–	
D	G5, 14 m	8 μM NO_2^- + 5 μM S^{2-}	0.21	0.13	1.61
E, F	G5, 14 m	16 μM NO_3^- + 15 μM H_2S*	0.8	0.56	1.42
G, H	G5, 14 m	8 μM NO_2^- + 15 μM H_2S*	0.26	0.17	1.52

for 48 h. Samples from all the bags were collected at every 3–6 h interval for NO_3^-, NO_2^-, H_2S and N_2O. NO_2^- was fixed by addition of a mixed reagent of sulphanilamide and N, N-Naphthyldiamine dihydrochloride (Grasshoff et al., 1999), and H_2S samples were immediately fixed as described in the Section 2.2. NO_3^- samples were preserved at 4 ℃, and N_2O samples were poisoned by adding 100 μL of saturated $HgCl_2$ solution.

2.6. Analysis

Dissolved O_2 samples were analyzed by Winkler titration after acidification of oxyhydroxide precipitates (Grasshoff et al., 1999). Nutrient samples were thawed to room temperature, mixed well and analyzed for NO_3^-, NH_4^+ and PO_4^{3-} colorimetrically using a Skalar Autoanalyzer following Grasshoff et al. (1999) within 24 h of collection with precisions ± 0.06, ±0.01, ±0.006 μM, respectively. H_2S and NO_2^- were determined onboard spectrophotometrically following Grasshoff et al. (1999) with precisions ± 0.14 μM and ± 0.02 μM, respectively. N_2O samples were analyzed by a Shimadzu Gas chromatograph equipped with ECD following Multiple Headspace analysis method (McAuliffe, 1971) with a precision of 4%.

Headspace samples were analyzed by a GC-IRMS (VG Optima) at the Max Plank Institute for Marine Microbiology (Bremen, Germany) for $^{29}N_2$ ($^{14}N^{15}N$), $^{30}N_2$ ($^{15}N^{15}N$), $^{45}N_2O$ ($^{14}N^{15}N^{16}O$) and $^{46}N_2O$ ($^{15}N^{15}N^{16}O$) following the method given by Holtappels et al. (2011) and Marchant et al. (2018). Prior to N_2O analysis, 25 μL of $^{44}N_2O$ standard (99.5%, Air Liquide, Germany) were added to samples to enhance the measurement sensitivity. Calibration for N_2 was done using air as a standard, and for N_2O, using the N_2O gas standard. For the determination of DNRA rates, the samples enriched with substrates $^{15}NO_2^-$ and $^{15}NO_2^- + S^{2-}$, were analyzed as follows. First, samples were sufficiently aerated to ensure complete removal of any dissolved ^{15}N-N_2. Then the samples were transferred to a 6 ml exetainers, degassed with Helium followed by the addition of 5 μM $^{14}NH_4^+$ and 200 μL of 4 M NaOBr (Warembourg et al., 1993; Preisler et al., 2007; Jensen et al., 2011). Then the samples were mixed well and 1 ml of He headspaces were created. ^{15}N-N_2 produced through the oxidation of $^{15}NH_4^+$ was analyzed as described before.

2.7. Rate calculation and statistical analysis

N deficit was calculated as $N^* = [DIN - (16 \times PO_4^{3-})] + 2.9$ as per Gruber and Sarmiento (2002)

where $DIN = NO_3^- + NO_2^- + NH_4^+$.

The rates of denitrification and anammox were calculated considering the linear increase in excess $^{29}N_2$ and excess $^{30}N_2$ in experiments with $^{15}NO_2^-$ enrichment following Thamdrup et al. (2006), Holtappels et al. (2011) and Dalsgaard et al. (2012) as given below.

$$N_{2\ anammox} = {}^{14}N^{15}N_{xs} \times (F_{NH4})^{-1} \text{ and}$$

$$N_{2\ denitrification} = {}^{15}N^{15}N_{xs} \times (F_{NO2})^{-2}$$

Where $^{14}N^{15}N_{xs}$ is the linear production rate of excess $^{14}N^{15}N$ i.e. $^{29}N_2$ with time,

$^{15}N^{15}N_{xs}$ is the linear production rate of excess $^{15}N^{15}N$ i.e. $^{30}N_2$ with time,

F_{NH4} is the mole fraction of ^{15}N in the NH_4^+ pool in the $^{15}NH_4^+$-amended incubations, and

F_{NO2} is the mole fraction of ^{15}N in the NO_2^- pool in the $^{15}NO_2^-$-amended incubations.

DNRA rate was calculated from the linear production rate of $^{15}NH_4^+$ derived from the measured ^{15}N-N_2 in the 6 ml exetainer vials as per Lam et al. (2009), Jensen et al. (2011), and De Brabandere et al. (2014) as follows

$$N_{DNRA} = {}^{14}N^{15}N_{xs} + (2\times\ {}^{15}N^{15}N_{xs})$$

By applying LINEST function (MS Excel) on the time plot of N_2, rates of denitrification, anammox and DNRA with standard deviation were calculated and presented in the Table 2 and figures (Figs. 4-6; Suppl. Figs. 3-10). As the contributions of anammox and DNRA were very low compared to denitrification, we did not take combined isotope effects taking the co-occurrence of all the processes into consideration (Song et al., 2016). To test the significance of variance between the data, ANOVA (MS Excel) was applied and variance was considered significant only where $p < 0.05$.

3. Results

3.1. Physical and biogeochemical condition over the shelf

During the study period, the shelf water column was vertically stratified, and the stratification was more prominent at the northern transects, as reported earlier (Naqvi et al., 2006, 2009; Shirodkar et al., 2018). Briefly, between Mumbai to Mangalore, a warm (27–29 °C), low saline (26–33 psu), low dense (σ_θ = 16–22 Kg m^{-3}), thin (2–7 m) oxic surface layer overlaid cold (22–25 °C), high saline (35–36 psu) suboxic/anoxic (0–4 μM O_2) subsurface water (Figs. 4, 5, 6). A relatively weaker vertical stratification was observed at Calicut where a colder (25–26 °C), higher saline (35 psu), denser (σ_θ = 23 Kg m^{-3}), thin (<1 m) oxic surface layer overlaid slightly colder 23 °C and denser (σ_θ = 23.9 Kg m^{-3}) anoxic (0 μM O_2) subsurface water that had the nearly same salinity as that of the surface layer (Fig. 6d). This indicated that upwelled water surfaced at Calicut (Rao et al., 2008; Gupta et al., 2016) whereas at the northern stations, upwelling was prevented by thermohaline stratification (Naqvi et al., 2006). However, the subsurface layer below the thermocline/pycnocline showed uniform physical characteristics down to the bottom at all stations (Figs. 4, 5, 6), presumably due to small scale vertical mixing induced by internal waves and/or upwelling (Unnikrishnan and Antony, 1990; Shenoi and Antony, 1991).

The intensity of O_2 deficiency varied across the shelf with more intense reducing conditions towards the coast (particularly off Goa, Mangalore and Calicut), leading to the co-occurrence of sulphidic condition (inner-shelf), suboxia (mid-shelf) and hypoxia (outer-shelf) (Fig. 3). On the inner shelf, the thickness of the oxic layer increased progressively from south to north, briefly the oxic layer was very thin (~5 m) at the Goa, Karwar, Mangalore and Calicut, and was comparably thicker (27 m) at the northernmost transect (Mumbai). Accordingly, the volume of the anoxic water mass decreased from south to north. Consequently, strong north–south biogeochemical gradients were observed in terms of O_2, H_2S, N*, N-nutrients, and N_2O (Fig. 7, Suppl. Fig. 2). The intensity of O_2 deficiency increased from north to south which was manifested in suboxia at the northern stations i.e. Mumbai and Karwar except Goa and euxinia at the southern stations, which apparently led to significant increase in N* and decrease in N-nutrients from north to south barring the exception at Goa (Fig. 7, Suppl. Fig. 2). Similarly, N_2O showed a decreasing trend from north to south with only an exceptional high at Mangalore (Suppl. Fig. 2).

The prevailing biogeochemical conditions in the bottom water clearly reflected 3 types of redox regimes over the WICS; (1) hypoxic bottom waters with measurable NO_3^-, low NO_2^- and low N_2O concentrations with a moderate to low N* signal i.e. at stations over mid- and outershelf, (2) suboxic bottom waters with low NO_3^- but high NO_2^- and N_2O concentrations combined with a substantial N* signal i.e. at B2, G6, K3 and M3, (3) anoxic bottom waters depleted in NO_3^- and NO_2^- with detectable sulphide (>0.1 μM) and high NH_4^+ i.e. at G3, G4, G5, M1 and C1 (Figs. 3, 4, 5, 6). On the Mumbai, Karwar and Mangalore transects, suboxia developed towards the coast, and NO_3^- dropped substantially while NO_2^- accumulated concomitant with the increase in N* (stations B1-B3, K2-K3, M1-M6) (Fig. 3), and except at M1, sulphide was not detected at any of these stations. The Goa transect exhibited all three

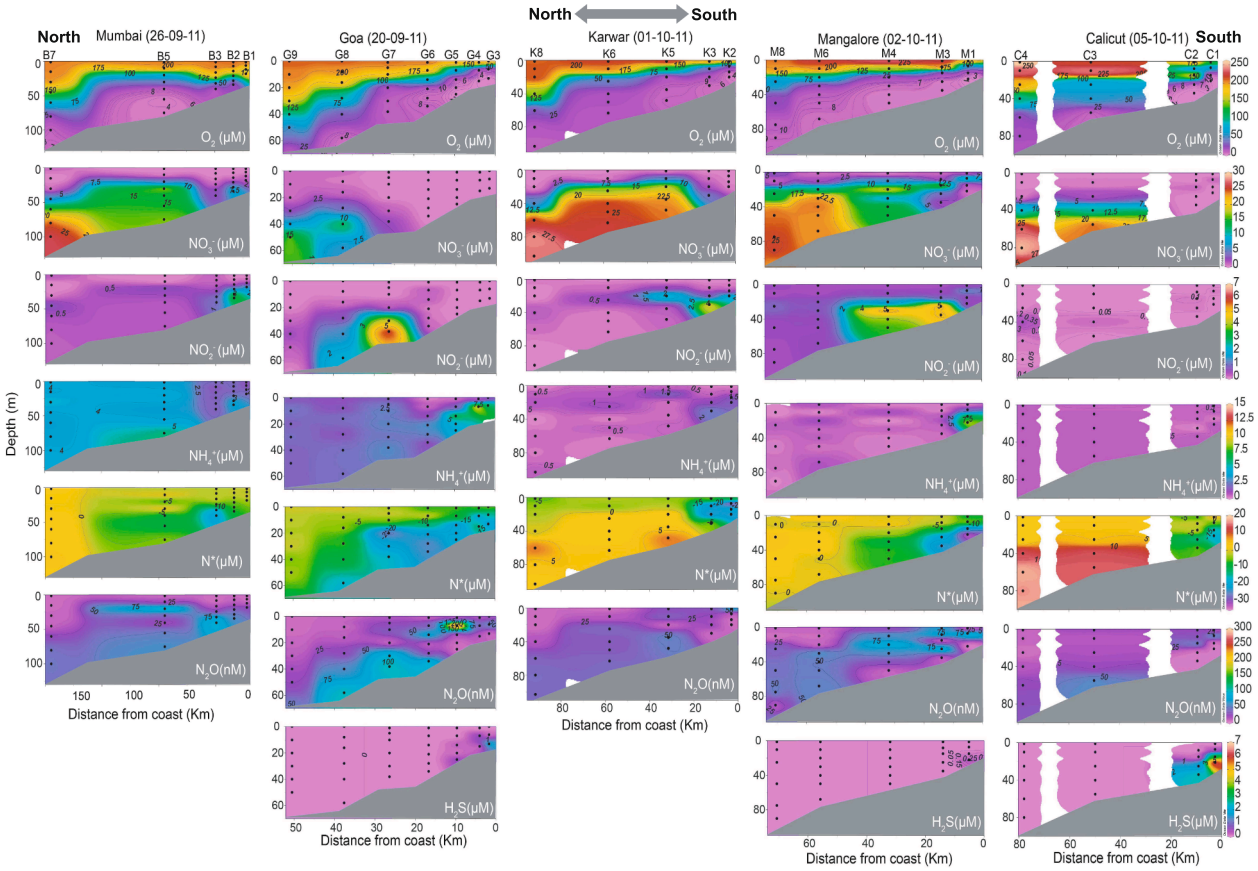

Fig. 3. Cross-shelf variation of biogeochemical parameters along the five transects off the Western Indian shelf. Some of the data from Mumbai, Goa, Mangalore and Calicut transect are taken from Bardhan and Naqvi (2020).

conditions, with hypoxic conditions on the outershelf (G8 and G9), suboxic conditions with high NO_2^- concentrations and N_2O accumulation on the mid shelf (G6-G7), and anoxic (sulphidic) conditions on the inner shelf (G3-G5). At Calicut, the bottom waters at stations C1 and C2 were sulphidic and depleted with NO_3^- and NO_2^-. At the station closest to the shore (C1), O_2 fell below detection at 7 m water depth and H_2S was detectable just below the oxic-anoxic interface, reaching concentrations of 6 μM in the bottom water (Fig. 6).

3.2. *Denitrification, N_2O, DNRA and anammox rates in the presence and absence of sulphide*

3.2.1. *Mumbai transect*

Incubations were carried out in the suboxic bottom water (34 m) at the station B2. The denitrification rate was moderate (261 nmol N_2 L^{-1} d^{-1}) in comparison to other stations (Fig. 4; Table 3) and was orders of magnitude higher than anammox rate. Furthermore, a transient accumulation of ^{15}N-N_2O was observed in the incubation ($^{45}N_2O$ and $^{46}N_2O$) (Suppl. Fig. 3a). Upon addition of sulphide, denitrification rates increased > 2 fold (Table 3; Fig. 4), and the transient accumulation of N_2O was substantially higher (Suppl. Fig. 3a). Furthermore, the addition of sulphide led to the occurrence of DNRA (Fig. 4; Table 3), although at rates orders of magnitude lower than denitrification.

3.2.2. *Goa transect*

At the stations with measurable sulphide on the Goa transect (G3, G4 and G5), incubations were carried out in the sulphidic bottom waters and just below the NO_x^--H_2S chemocline where NO_2^- concentrations peaked and sulphide dropped below detection. At G5, incubations were also carried out at an additional depth located between the bottom water and the chemocline (Fig. 5). Denitrification was the dominant process at all depths (221–2921 nM N_2 d^{-1}), followed by DNRA (5.3–45 nM N d^{-1}) and anammox (0–41 nM N_2 d^{-1}) (Fig. 5; Table 3). At the depth below the chemocline of G3 (6 m), G4 (7 m) and G5 (14 m) or in the G3 bottom water (13 m), sulphide addition had no significant effect on denitrification rates ($p = 0.79$) but did stimulate rates in the bottom water of G4 (15 m) and G5 (20 m and 25 m) significantly ($p = 0.02$). Sulphide addition significantly stimulated DNRA rates in all the incubations ($p = 0.002$) with the exception of the oxic-anoxic interface at G3 (6 m) and G5 bottom water (25 m) ($p = 0.85$). At G6, where no NO_3^- or sulphide was measurable in the water column, incubations were carried out below the oxic-suboxic interface where nitrite was undetectable (28 m) and in the bottom water (34 m) where NO_2^- peaked. The denitrification rate ranged from 104 nM N_2 d^{-1} at 28 m and 901 nM N_2 d^{-1} at 34 m. No DNRA was detected at 28 m, but a rate of 7.2 nM N d^{-1} could be detected at 34 m, which was the lowest DNRA rate measured during this study. Similarly, anammox rates were very low at 28 m (1.5 nM N_2 d^{-1}) and rose to 27 nM N_2 d^{-1} at 35 m. The addition of sulphide led to an increase in denitrification rates by more than an order of magnitude at 28 m but by ~ 3 fold at 34 m. Sulphide addition led to measureable DNRA rates at 28 m and doubled the rate at 35 m. At all the stations on the Goa transect, a transient production of ^{15}N-N_2O was observed, and with sulphide addition, this intermediate ^{15}N-N_2O production increased substantially at all stations off Goa (Suppl. Fig. 3b, 4, 5, 6 and 7).

3.2.3. *Karwar transect*

Incubations were carried out at station K3 on the Karwar transect at just below the oxic-suboxic interface (20 m) and in the bottom water (30 m). At K3, bottom water was non-sulphidic with high NO_x^- and NH_4^+ concentrations. Denitrification was the dominant process at both the depths (264–408 nM N_2 d^{-1}) followed by anammox (6.5–33 nM N_2 d^{-1}) and DNRA (8–30 nM N d^{-1}) (Fig. 6a; Table 3). Upon the sulphide

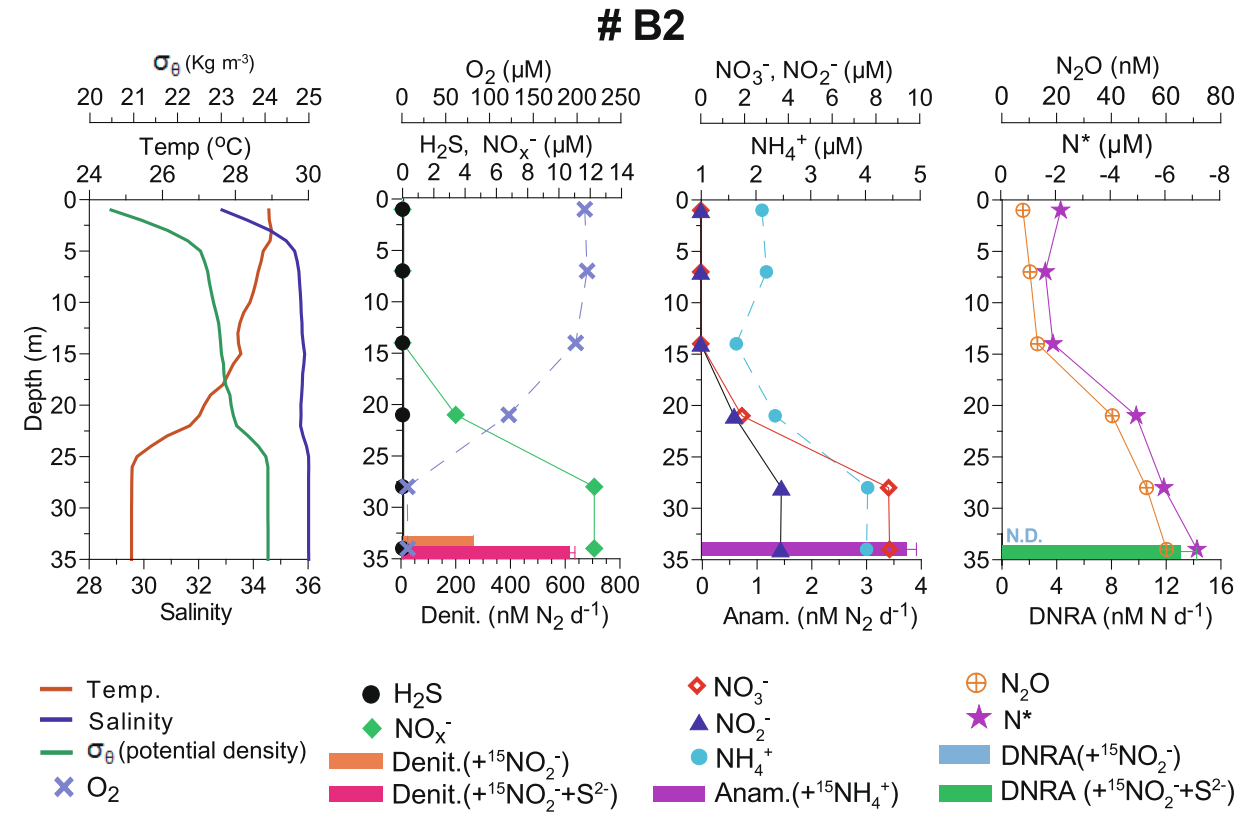

Fig.4. Physico-chemical condition and N transformation rates at station B2, off Mumbai. Denit.: Denitrification, Anam.: anammox, N.D.: not detected.

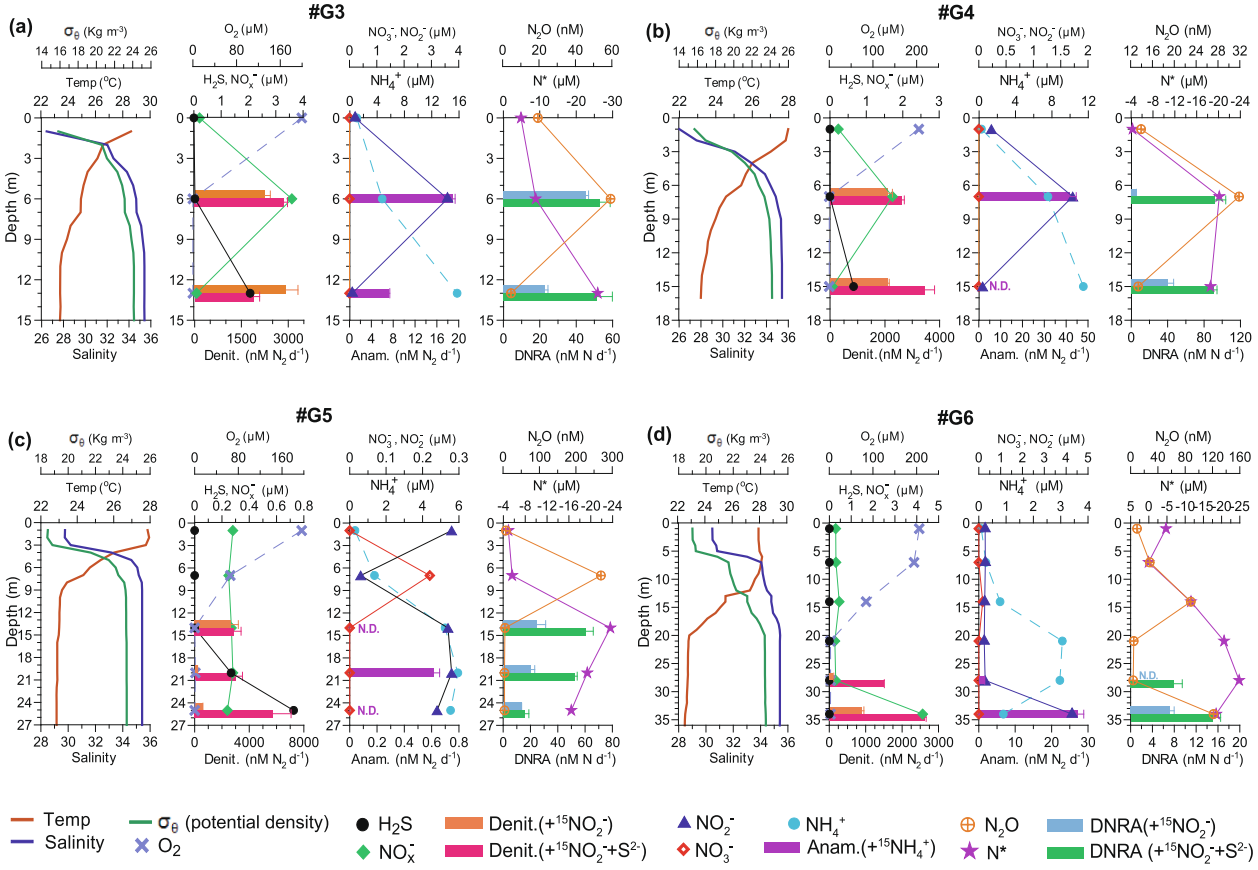

Fig. 5. Physico-chemical condition and N transformation rates at stationsG3, G4, G5 and G6, off Goa. Denit.:Denitrification, Anam.: anammox, N.D.: not detected.

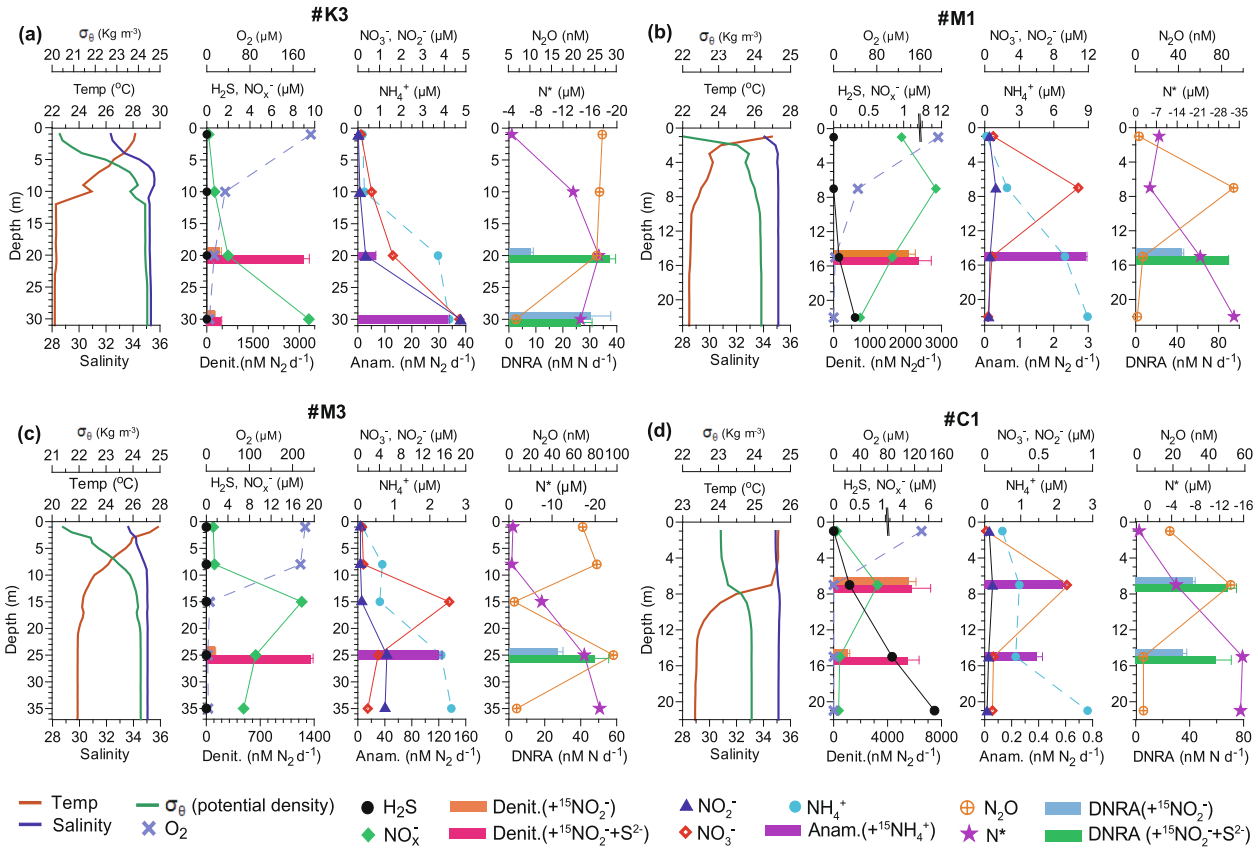

Fig. 6. Physico-chemical condition and N transformation rates at stations K3 (off Karwar), M1 and M3 (off Mangalore), and C1 (off Calicut). Denit.: Denitrification, Anam.: anammox, N.D.: not detected.

addition, denitrification was stimulated by 7.6 fold at 20 m and 1.7 fold at 30 m. Sulphide addition led to 4.5 fold increase in DNRA rate at 20 m but no stimulation was observed at 30 m. Transient accumulation of N_2O was observed during the incubation although not very prominently at 20 m. However, sulphide addition significantly stimulated N_2O accumulation at both the depths (Suppl. Fig. 8).

3.2.4. *Mangalore transect*

Incubations on the Mangalore transect were carried out at two stations (M1 and M3). At station M1, where the bottom water was depleted in NO_3^- and NO_2^- but H_2S was detectable, incubations were carried out at just below the NO_x^--H_2S chemocline (15 m). The denitrification rate (2079 nM N_2 d^{-1}) was much higher than the DNRA and anammox rate (Fig. 6b, Table 3) and was associated with a transient production of N_2O (Suppl. Fig. 9a). Upon addition of sulphide, there was no significant increase in denitrification rate, but there was a higher transient production of N_2O, and DNRA rates doubled. Station M3 still had measureable NO_3^- and NO_2^- in the bottom water but no H_2S (Fig. 6c), and incubations were carried out at 25 m. In the incubations without added sulphide, the denitrification rate (114 nM N_2 d^{-1}) was nearly same as anammox rate (119 nM N_2 d^{-1}) but higher than DNRA (27 nM N d^{-1}), and a transient peak of N_2O accumulation was observed (Suppl. Fig. 9b). The addition of sulphide caused denitrification to increase by an order of magnitude (1358 nM N_2 d^{-1}), DNRA to double and led to a steady accumulation of N_2O.

3.2.5. *Calicut transect*

The incubations on the Calicut transect were carried out at station C1, at a depth just below the oxic-anoxic interface (7 m) and in the bottom water (15 m) which were NO_x^- depleted, sulphidic and had NH_4^+ concentrations up to 2.5 μM (Fig. 6d). At the oxic-anoxic interface, the denitrification rate was 5825 nM N_2 d^{-1}, which was the highest rate measured at any station with no added sulphide in the incubation (Table 3; Fig. 6d). The DNRA rate (40 nM N d^{-1}) was similar to that at the other stations (Table 2), and anammox rates were extremely low (0.58 nM N_2 d^{-1}). At 15 m, denitrification still dominated over DNRA and anammox but the rates were 5 times lower than that at 7 m (Table 3). Upon addition of sulphide, no discernible increase was observed in the denitrification rate at 7 m, but it increased 5 fold to 5518 nM N_2 d^{-1} at 15 m, and 2 fold increases in DNRA rates at both the depths. Sulphide addition also led to higher transient production of N_2O at both the depths (Suppl. fig. 10).

3.3. *Variability of N loss/transformation rates along the shelf*

Depth-integrated denitrification, anammox and DNRA rates exhibited significant variability from north to south over the shelf (Fig. 7) in response to variability in O_2 deficiency and N-nutrient availability. The denitrification rate showed an overall increase from Mumbai to Calicut, apart from at Karwar, and there was a trend of increasing denitrification rate with S^{2-} addition from north to south with higher rates (with the exception of a decrease at Mangalore). No regular trend in the anammox rate was observed from north to south; rather it increased from north to a maximum at Mangalore and further decreased towards south. A clear increasing trend in the DNRA rate was noticed from north to south, and furthermore, with S^{2-} addition, the DNRA rates increased but the trend remained the same.

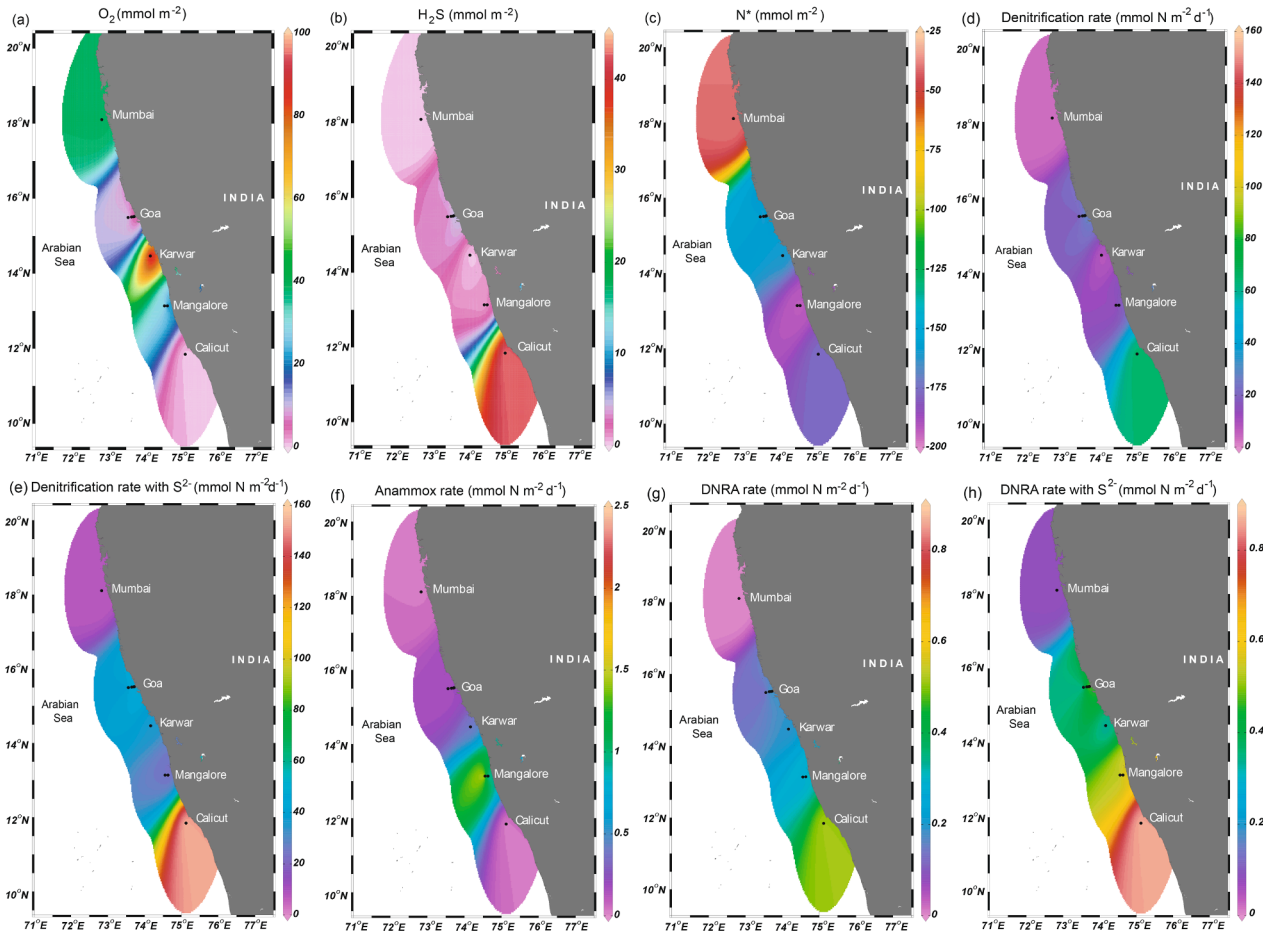

Fig. 7. Spatial variability of depth-integrated O_2, H_2S, N-deficit, denitrification, anammox and DNRA rates in the subsurface waters of WICS during the study period.

Table 3
N transformation rates with standard deviation (in parenthesis) in the shelf waters of western India as determined through ^{15}N-incubations.

Station	Depth (m)	Denitrification (nmol N_2 L^{-1} d^{-1})	Denitrification with S^{2-} (nmol N_2 L^{-1} d^{-1})	Anammox (nmol N_2 L^{-1} d^{-1})	DNRA (nmol N L^{-1} d^{-1})	DNRA with S^{2-} (nmol N L^{-1} d^{-1})
B2	34	261 (±2.8)	615 (±19)	3.7 (±0.18)	n.d.	14 (±1.1)
G3	6	2242 (±184)	2860 (±114)	18.8 (±0.45)	45 (±1.4)	53 (±5.5)
	13	2921 (±388)	1885 (±197)	7.1 (±0.22)	22 (±1.9)	51 (±8.7)
G4	7	2106 (±165)	2608 (±100)	41 (±2.9)	5.3 (±0.39)	91 (±12)
	15	2120 (±37)	3455 (±359)	n.d.	40 (±6.4)	90 (±3.8)
G5	14	2646 (±551)	2880 (±520)	n.d.	24 (±6.4)	60 (±5.3)
	20	221 (±6.8)	2990 (±515)	0.61 (±0.04)	19 (±3.2)	52 (±2.1)
	25	544 (±78)	3081 (±470)	n.d.	13 (±0.13)	15 (±3)
G6	28	104 (±18)	1495 (±14)	1.5 (±0.08)	n.d.	7.9 (±1.5)
	34	901 (±50)	2615 (±45)	27 (±1.5)	7.2 (±0.75)	15 (±1.4)
K3	20	408 (±63)	3137 (±187)	6.5 (±0.17)	8.1 (±0.91)	37 (±2.2)
	30	264 (±5.5)	460 (±23)	33 (±0.6)	30 (±7.6)	26 (±4.3)
M1	15	2079 (±192)	2365 (±350)	2.9 (±0.02)	44 (±2.1)	89 (±0.34)
M3	25	114 (±7.9)	1358 (±26)	119 (±5.4)	27 (±2.8)	47 (±7.8)
C1	7	5573 (±531)	5825 (±1363)	0.58 (±0.02)	40 (±1.4)	68 (±6.1)
	15	1087 (±104)	5518 (±817)	0.38 (±0.04)	35 (±2.6)	59 (±11)

3.4. NO_x^- reduction, sulphide oxidation, and N_2O build-up in the bag incubations

Bag incubations of the chemocline waters from stations G5 (14 m) and G6 (28 m) showed similar results. In the Bags A-D, NO_2^- decreased linearly over time and a transient accumulation of N_2O was observed (Fig. 8). Relative to the incubations with only added NO_2^- (Bag A and C), in the incubations with added NO_2^-+S^{2-} (Bag B and D), NO_2^- consumption rates (Table 2) were higher, and N_2O accumulated faster and to higher concentrations until net consumption began (Fig. 8). NO_2^- and sulphide were both consumed linearly in a ratio of 1.61–1.78 (Table 3). Similar pattern of NO_2^- reduction, S^{2-} oxidation and N_2O production/consumption at both G5 and G6 indicated that the results could be replicated at different stations. In the Bags E and F (native sulphide + NO_3^-), no appreciable change in NO_3^- and H_2S concentrations occurred for the first 6 h, after which a rapid simultaneous decrease in the concentrations of both occurred until 24 h (Fig. 8) at a ratio of 1.42 (Table 3). NO_2^- accumulated after 6 h and peaked up to 13 μM at 24 h followed by a steady decrease. A rise in N_2O was observed from 0 h until 24 h after which concentrations increased steeply, peaking to 125 nM at

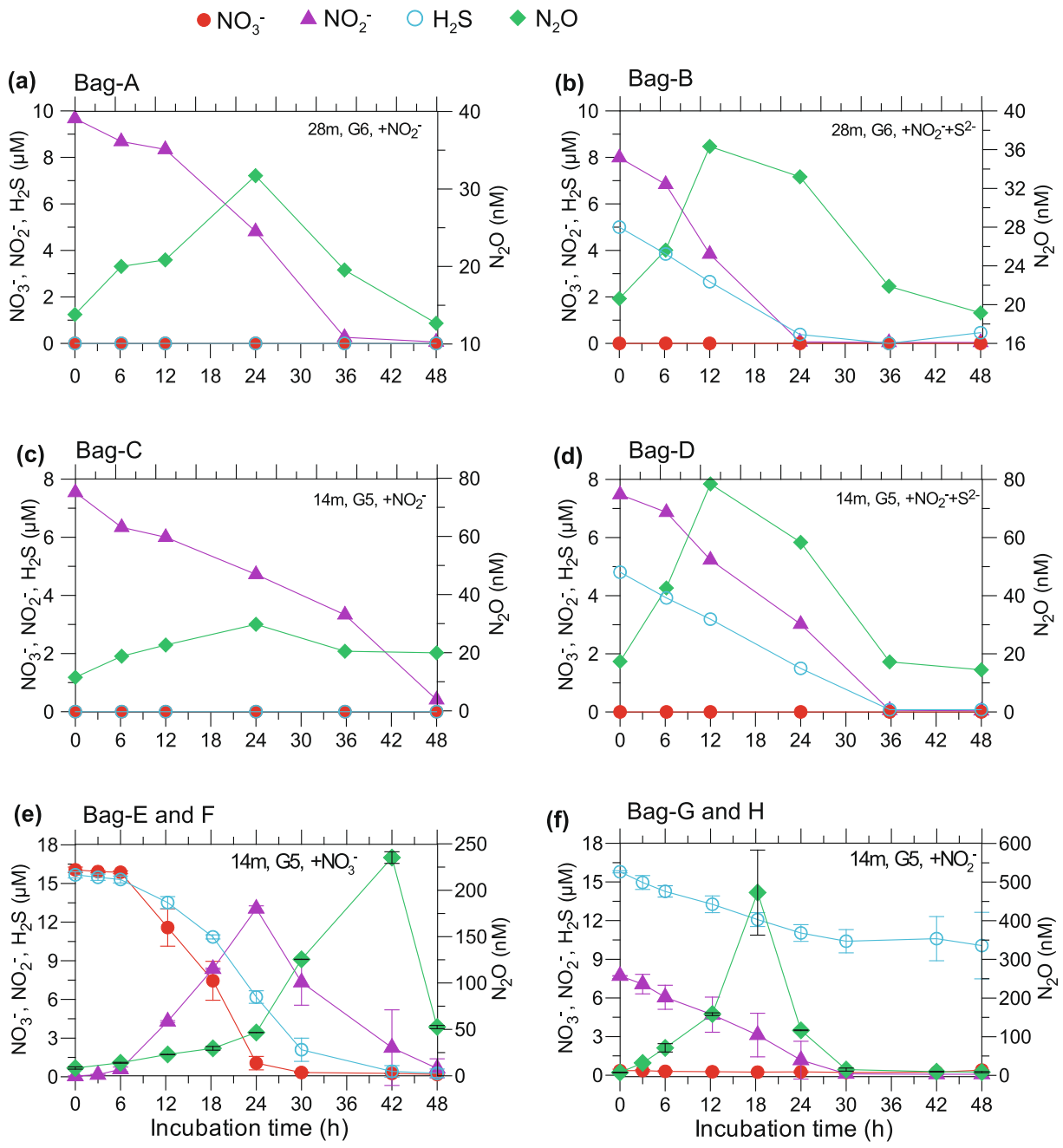

Fig. 8. Incubation of water from the suboxic-anoxic interface at G6 (a) with added NO_2^- and (b) with added NO_2^-+S^{2-}; incubation of water from the suboxic-anoxic interface at G5 (c) with added NO_2^- and (d) with added NO_2^-+S^{2-}; incubation of water from suboxic-anoxic interface at G5 after ~ 2 weeks of pre-incubation (e) mean results of bag E and F spiked with NO_3^- (f) mean results of bag G and H spiked with NO_2^-.

42 h and decreasing rapidly afterwards. There was no statistically significant variance in the experimental results between the two bags (n = 9, $p > 0.7$; ANOVA) indicating good reproducibility. In the Bags G and H (native sulphide + NO_2^-), NO_2^- and H_2S decreased simultaneously at a ratio of 1.52 (Table 3) and N_2O started increasing steadily from 0 h (Fig. 8). NO_2^- was undetectable after 30 h but 9–12 μM of H_2S remained at the end of the experiment. A sharp increase in N_2O concentrations was observed after 12 h, peaking up to 472 nM at 18 h followed by a rapid decrease. Concentration change patterns between in the two bags did not vary significantly (n = 9, $p > 0.2$; ANOVA) implying a good replication of the results. The mean consumption rates of NO_2^- and S^{2-} derived from the Bags B, D, G and H were 0.27 ± 0.07 μmol N L^{-1} h^{-1} and 0.16 ± 0.03 μmol L^{-1} h^{-1}, respectively, and the mean consumption ratio of NO_2^- to S^{2-} was 1.58. Overall, the bag incubation of the chemocline waters from both G6 and G5 showed simultaneous NO_x^- reduction and S^{2-} oxidation along with transient N_2O production, indicating that the NO_x^- reduction to N_2 was coupled to the oxidation of native or added sulphide, and that both NO_x^- reduction and N_2O production are stimulated by increasing sulphide level.

4. Discussion

4.1. Signatures of N-loss, and build-up of N_2O and H_2S

During the study period, the prevailing biogeochemical characteristics of the WICS waters indicated suboxia at stations B2, G6, K3 and M3, and anoxia at stations G3, G4, G5, M1 and C1, since the subsurface waters at the former stations were sulphide-free and NO_x^--replete

whereas the subsurface waters at the latter stations were sulphidic and NO_x^--depleted (Figs. 4, 5, 6). The intensity of O_2 deficiency, OMZ thickness, NO_x^- concentrations and N* indicated N-loss which increased southward. Such observations are in line with the patterns previously observed during the southwest monsoon season (Naqvi et al., 2006; Bardhan and Naqvi, 2020; Sarkar et al., 2020). At the stations closest to the coast over Goa, Mangalore and Calicut transect i.e. G3, G4, G5, M1 and C1, the bottom waters were nearly depleted in NO_x^-, and exhibited higher N* values and detectable sulphide (Figs. 5, 6) compared to the stations farther from the coast (Fig. 3). In contrast, at the stations closest to the coast on the Mumbai and Karwar transects (B2 and K3), and G6 and M3, there was a prominent NO_2^- accumulation and relatively lower N* (Figs. 4, 5, 6). Together these results indicated that denitrification was occurring at the above four stations, but was less advanced than that at the sulphidic stations. Interestingly, the pattern of N_2O accumulation differed between the sulphidic and non-sulphidic stations. At the non-sulphidic stations (e.g. B2, G6, K3, M3), the highest N_2O concentration was observed within the OMZ core and lower N_2O was observed at the oxic-anoxic interface (Figs. 4, 5d, 6c). In contrast, at the sulphidic stations (e.g. G3, G4, G5, M1, and C1), the opposite was true i.e. the N_2O peak was observed at or just above the oxic-anoxic interface, and was depleted within the core of OMZ (Fig. 5a-c, 6b, d). At the sulphidic stations, a clear overlapping of NO_x^- and H_2S profiles was conspicuous wherein substantial NO_x^- concentration (0.27–3.6 μM) was detected at the oxic-anoxic interface, which decreased further down to the bottom (Figs. 5, 6). Even the near bottom sulphidic water contained some traces of NO_x^- (0.1–0.86 μM) which clearly indicated the mixing of NO_x^--replete suboxic water with underlying sulphidic water. Co-existence of NO_x^- and H_2S occurred possibly due to (1) the small scale vertical mixing via turbulent motions induced by internal waves (Unnikrishnan and Antony, 1990; Shenoi and Antony, 1991) as also observed in the Baltic Sea (Hannig et al., 2007; Dalsgaard et al., 2013) and/or (2) the vertical movement of water caused by upwelling (Unnikrishnan and Antony, 1990). This was substantiated by the uniformity of σ_θ from the oxic-anoxic interface to the bottom at these stations (Fig. 5a, b, c; Fig. 6b, d). The thickness of the mixing zone of NO_x^- and H_2S i.e. *substrate mixing zone* (SMZ) varied from 7 to 15 m at the sulphidic stations with an average of 11 m.

4.2. Impact of sulphide on anammox and DNRA rates

Anammox was detected at most sampled stations and depths, with a maximum rate of 119 nM N_2 d^{-1} at station M3 (Fig. 6c; Table 3). Previously, Naqvi et al. (2006) suggested a high potential for anammox activity in the shelf waters during seasonal anoxia as the benthic-released NH_4^+ (Pratihary et al., 2014) can enter the overlying NO_2^--rich bottom water. We observed higher anammox rates i.e. 1.5–119 nM N_2 d^{-1} at the non-sulphidic stations compared to the sulphidic stations where anammox occurred at the rates 0–41 nM N_2 d^{-1}. Particularly, in the sulphidic bottom waters, anammox rates were extremely low (0–7 nM N_2 d^{-1}) often being below detection. Our observation is consistent with Sarkar et al. (2020) who previously reported higher average anammox rates in the shelf waters during suboxic (non-sulphidic) events (70 nM N_2 d^{-1}) compared to sulphidic events wherein anammox was below detection. These observations indicate that the sulphidic event apparently suppressed the anammox activity in the shelf waters as also observed in other coastal systems (Dalsgaard et al., 2003; Jensen et al., 2008). Thus, we believe that anammox was possibly more prominent during the early phase of seasonal anoxia over the shelf (July-August) owing to sufficient NO_x^- availability and absence of sulphide, and with the intensification of anoxia, it decreased substantially often being undetectable.

Accumulation of $^{15}NH_4^+$ in the $^{15}NO_2^-$ labeled incubations suggested that a part of the added NO_2^- was reduced to NH_4^+ via DNRA. Like anammox, DNRA was detected at most depths and stations at rates 0–45 nM N d^{-1}, almost in the similar range of anammox rates. Particularly, it occurred at relatively higher rates (5.3–45 nM N d^{-1}) at the sulphidic depths compared to non-sulphidic depths (0–30 nM N d^{-1}) ($p = 0.02$). Moreover, the addition of sulphide to incubations led to a significant increase (1.17–17 times) in DNRA rates at 13 out of 16 depths tested. In fact, at B2 (34 m), and G6 (28 m), DNRA was detectable only after addition of sulphide. Sarkar et al. (2020) also reported higher DNRA rates in the shelf waters during anoxia than during suboxia wherein DNRA was mostly undetectable. These observations suggested that the DNRA in the shelf waters was largely sulphide-driven (Eq. 3) as also observed in other coastal marine systems (Hannig et al., 2007; Bernard et al., 2015; Bonaglia et al., 2016).

$$HS^- + NO_3^- + H^+ + H_2O \rightarrow NH_4^+ + SO_4^{2-} \quad (3)$$

(Burgin and Hamilton, 2008)

4.3. Evidence for sulphide-driven (chemolithotrophic) denitrification

By and large, denitrification was found to be the dominant process at all stations with the only exception at M3 (25 m) where it was marginally exceeded by the anammox (Table 3). Previously, Sarkar et al. (2020) have reported higher denitrification rates (mean = 3.2 μmol N_2 L^{-1} d^{-1}) in the WICS waters during a sulphidic year (2009) than during two non-sulphidic years (mean = 1.53 μmol N_2 L^{-1} d^{-1}; 2008 and 2010), and they hypothesized that the higher denitrification rate during anoxia was due to the effect of sulphide. We observed that denitrification rates were generally higher in water sampled from sulphidic stations and depths (G3, G4, G5, M1 and C1; 221–5773 nmol N_2 L^{-1} d^{-1}) than in those from non-sulphidic stations and depths (B2, G6, K3 and M3; 104–901 nmol N_2 L^{-1} d^{-1}) (Table 3). Furthermore, denitrification rates increased significantly (1.6–14 times) upon sulphide addition in 10 out of 16 depths ($p = 0.006$), and the magnitude by which they increased appeared to be related to the in-situ sulphide concentrations, i.e. there was a stronger increase in denitrification rates upon sulphide addition in samples from the non-sulphidic waters (1.7–14 times), compared to those from already sulphidic waters (0.65–13 times). In contrast, just below chemocline of the sulphidic stations, no significant increase in denitrification rate (1.05–1.28 times) was observed with added $^{15}NO_2^- + S^{2-}$ compared to that with only $^{15}NO_2^-$ addition ($p = 0.69$). This indicated that the growth of denitrifiers at these stations was possibly already near saturation with respect to the native sulphide level which led to a marginal enhancement in the denitrification rates upon extra sulphide addition. Moreover, the bag incubations of the chemocline waters from both suboxic and anoxic stations (Fig. 8) showed that the NO_x^- reduction and transient N_2O production were coupled to sulphide oxidation, and were stimulated by increasing sulphide level, as also observed elsewhere (Jensen et al., 2009; Dalsgaard et al., 2013; Galán et al., 2014).

We also observed the elemental sulphur plumes adjacent to the reported sulphidic waters of WICS, which are also indicative of chemolithotrophic sulphide oxidation coupled with denitrification, as observed in other euxinic coastal systems (Schunck et al., 2013; Callbeck et al., 2018; Ohde, 2018; Ohde and Dadou, 2018). However, detection of S^0 plume only at the southern transect (near Calicut) rather than at the northern transects indicated that the upwelling of chemolithotrophically produced S^0 in the subsurface waters is prevented at the latter transects. During South-west monsoon, the upwelled water is known to surface off Southwest Indian coast (Rao et al., 2008; Gupta et al., 2016; Kamaleson et al., 2019) but this does not occur off northern part of Indian west coast as a strong pycnocline prevents the entrainment of subsurface water to surface (Naqvi et al., 2006). This is also evident from the contrasting vertical profiles of temperature and salinity between C1 (Calicut), and B2 (off Mumbai), (G3-G6) off Goa, K3 (off Karwar) and (M1, M3) off Mangalore (Figs. 4-6). At the latter four transects, there is a warm (>26° C), low saline (<34) water layer at the surface whereas at C1, the surface layer is cooler (<26° C) and more saline (~35). Thus, the upwelled

water apparently surfaced at C1, which was not the case at the northern stations, which caused a part of S^0 pool surfaced as plumes near off Calicut whereas it got oxidized to SO_4^{2-} within the subsurface anoxic depths at Mangalore, Karwar, Goa and Mumbai. However, it only indicated that at C1, the rate of S^0 accumulation (at surface) exceeded its oxidation to SO_4^{2-}, and did not rule out the oxidation of the rest of S^0 to SO_4^{2-} in the subsurface waters.

To further investigate the response of denitrification to sulphide, we tested denitrification rates as a function of sulphide concentration (Suppl. fig. 11) wherein we observed a strong positive correlation ($r^2 > 0.9$) between denitrification rate and sulphide concentration at 5 depths, with the rates attaining maxima at 10 μM S^{2-}. But at most of the depths, we observed the denitrification rates either reaching maxima at 5 μM S^{2-} or increasing non-linearly or decreasing beyond that as also observed elsewhere (Hietanen et al., 2012). Similar sulphide dependency of denitrification has been reported in other anoxic costal systems as well (Jensen et al., 2009; Dalsgaard et al., 2013; Galán et al., 2014; Michiels et al., 2019). These results indicated that the denitrification in the WICS waters was stimulated by sulphide up to 5–10 μM beyond which it was either saturated or inhibited. The response of denitrification to increasing sulphide levels can vary among various systems due to specific adaptive capability of a particular group of denitrifiers to a specific physico-biogeochemical condition of the system (Bonaglia et al., 2016). For instance, Dalsgaard et al. (2013) and Jensen et al. (2009) did not observe any saturation or inhibition in denitrification up to 10 μM and 40 μM sulphide, respectively, whereas Bonaglia et al. (2016) reported a saturation or inhibition in denitrification at ≥ 2 μM sulphide which was due to the inhibition of the reductase enzyme catalyzing the last step of denitrification.

During September-October, colorless sulphur-oxidizing bacteria (Kamaleson et al., 2019) and particularly, *Thiobacillus denitrificans* like organism (Krishnan et al., 2008), a sulphur-oxidizing denitrifier belonging to β-proteobacteria prevail in the suboxic/anoxic subsurface waters of the WICS. More recent studies have detected a culturable sulphur-oxidizing denitrifiers such as *Marinobacter hydrocarbonoclasticus* (Gomes et al., 2020) and other sulphur-oxidizing denitrifiers belonging to clade SUP05, and groups *Thiomicrorhabdus* sp., *Marinobacterium* sp., *Alcanivorax* sp. and *Vibrio* sp. in the suboxic/anoxic WICS waters through V3-V4 sequencing of the 16S rRNA (Naik et al., in preparation). Hence, our combined results from in-situ rate experiments, bag incubations, sulphur plume imaging and detection of sulphur-oxidizing chemoautotrophic denitrifiers strongly indicated that that the denitrification over the WICS was largely driven and/or stimulated by sulphide, being carried out by sulphur-oxidizing chemolithotrophs in the anoxic WICS waters.

4.4. Relative contribution of chemoorganotrophic and chemolithotrophic (sulphide-driven) denitrification

Although we have strong evidence that sulphide-driven denitrification was occurring, we cannot exclude that there was co-occuring non-sulphide-driven denitrification i.e. chemoorganotrophic denitrification coupled to organic matter oxidation. Previous studies based on PCR amplification of nirS and nirK genes, and DNA sequencing have revealed the presence of a diverse, presumably chemoorganotrophic denitrifiers dominating the suboxic shelf waters during the early phase of denitrification (July-August) (Jayakumar et al., 2004; Gomes et al., 2018). The occurrence of chemoorganotrophic denitrification during August has also been observed based on its biogeochemical signatures in the bag incubation (Naqvi et al., 2000) and ^{15}N-labeled incubation (Sarkar et al., 2020) of the NO_x^--rich suboxic (sulphide-free) shelf waters. Therefore, based on the prevailing biogeochemical conditions at stations B2, G6, K3, and M3, where the water column was suboxic (i.e. sulphide-free and NO_x^--replete), all of the denitrification in the experiments with only $^{15}NO_2^-$ addition appears to be chemoorganotrophic with a mean rate of 342 (±296) nmol N_2 L^{-1} d^{-1}. In a very similar case, Dalsgaard et al. (2013) and Bonaglia et al. (2016) experimentally showed the occurrence of chemoorganotrophic denitrification within the NO_x^--replete, sulphide-free chemocline of the Baltic Sea. However, the stimulation in denitrification rates by 1.7–14 folds at these suboxic stations upon $^{15}NO_2^-$+S^{2-} addition indicated (1) the presence of sulphide-oxidizing denitrifiers in the suboxic waters and (2) the potential occurrence of sulphide-driven denitrification up to rates of 1613 (±1070) nmol N_2 L^{-1} d^{-1}. Since our sampling period was only up to 1st week of October, we did not observe sulphidic condition at these stations which are otherwise known to turn sulphidic during October (Naqvi et al., 2000, 2006, 2009; Shirodkar et al., 2018; Sarkar et al., 2020), whereupon we speculate that sulphide would stimulate the denitrification rate.

Although, H_2S in the WICS waters is known to vary spatially and annually, the average of the maximum H_2S concentration reported from a decade long observation (Naqvi et al., 2009) can be considered as ~ 5 μM which is close to the maximum H_2S observed in our study i.e. 6 μM. Therefore, the denitrification rates observed with $^{15}NO_2^-$+5 μM S^{2-} addition can closely represent the actual/potential sulphide-driven denitrification rates in the shelf waters. Precisely, at the sulphidic stations (i.e. G3, G4, G5, M1 and C1), the rates (mean: 3347 ± 1298 nmol N_2 L^{-1} d^{-1}) can be considered as the actual denitrification rates whereas at the suboxic stations (i.e. B2, G6, K3 and M3), the rates (mean: 1614 ± 1070 nmol N_2 L^{-1} d^{-1}) can be considered as the potential denitrification rates. Considering the rates at all the stations and depths, the mean rate of sulphide-driven denitrification was observed to be 2697 (±1464) nmol N_2 L^{-1} d^{-1} whereas anammox and DNRA occurred at the mean rates of 16.5 nmol N_2 L^{-1} d^{-1} and 48.7 nmol N L^{-1} d^{-1}, respectively. This showed that our mean actual sulphide-driven denitrification rate (i.e. 3.34 μM N_2 d^{-1}) was very similar to the denitrification rate (i.e. 3.21 μM N_2 d^{-1}) reported by Sarkar et al. (2020) during the sulphidic event of 2009. A comparative analysis of the sulphide-driven denitrification rates, anammox and DNRA rates among the anoxic coastal systems of the world (Table 4) shows that the highest sulphide-driven denitrification rate we observed over the WICS (11650 nmol N L^{-1} d^{-1}, off Calicut) is one of the highest in the world, being second only to the rate observed in the Mariager Fjord (37200 nmol N L^{-1} d^{-1}; Jensen et al., 2009). Considering our mean rate of chemoorganotrophic denitrification as 342 (±296) nmol N_2 L^{-1} d^{-1} observed at the suboxic stations and the denitrification rate reported by Sarkar et al. (2020) during suboxic years (i.e. 1.53 μM N_2 d^{-1}), it appears that with the advent of sulphidic event, chemolithoautotrophic denitrification replaces chemoorganotrophic denitrification as the dominant N loss process and causes massive N loss at a rate 2–8 times faster than that via chemoorganotrophic denitrification over the WICS.

4.5. Optimum, limitation and sustenance of chemolithoautotrophic denitrification

During September, the prevailing shelf biogeochemistry primes the condition for the occurrence of sulphide-driven denitrification as the suboxic water column still carries a modest amount of NO_x^- (mainly NO_2^-), and receives significant sulphide flux from the sediments (i.e. 4.3 mmol m^{-2} d^{-1}; Pratihary et al., 2014). The vertical velocity of upwelling over the WICS i.e. 2.77 × 10^{-2} cm s^{-1} (Unnikrishnan and Antony, 1990) suggests that the benthic-released sulphide would result in sulphide accumulation at the rate of 0.39 μmol L^{-1} d^{-1} in the 11 m-thick SMZ. The pelagic sulphide generation rate i.e. 1.17 μmol L^{-1} d^{-1} (Pratihary et al., in preparation) would further increase the total sulphide accumulation rate to 1.56 μmol L^{-1} d^{-1}. But the sulphide oxidation rate measured from the bag incubations i.e. 3.84 μmol L^{-1} d^{-1} (Section 3.4) or estimated from the mean sulphide-driven denitrification rate (2.69 μM N_2 d^{-1}) using HS^-:N_2 ratio (Eq. 1) i.e. 3.37 μmol L^{-1} d^{-1} was > 2 fold higher than the sulphide accumulation rate. Consistently, Kamaleson et al. (2019) have reported much higher rates of sulphur-oxidizing activity (SOA) than sulfate-reducing activity (SRA) in the near-suboxic

Table 4
A comparison of the rates of chemolithoautotrophic denitrification, anammox and DNRA along with the highest H_2S observed in various anoxic coastal systems of the world. n.d.: not detected, n.m.: not measured.

Coastal system, Location	Maximum H_2S (μM)	Chemolithoautotrophic denitrification (nM N d^{-1})	Anammox (nM N d^{-1})	DNRA (nM N d^{-1})	Reference
Golfo Dulce Bay, Costa Rica	1.8	48–5184	72–450	n.m.	Dalsgaard et al. (2003)
Baltic Sea	110	100–5400	10–100	20–510	Hannig et al. (2007)
	62	440–9318	10–18	n.m.	Hietanen et al. (2012)
	40	11–763	n.d.	n.m.	Dalsgaard et al. 2013)
	175	490–3813	1.7–7.4	100–432	Bonaglia et al. (2016)
Mariager Fjord, Denmark	277	100–37200	n.d.	n.m.	Jensen et al. (2009)
Namibian Shelf	18	n.d.-560	n.d.-140	n.m.	Lavik et al. (2009)
Peruvian Shelf	4.2	33–490	50–250	4–40	Schunck et al. (2013)
Chilean Shelf	~15	n.d.–2322	n.d.-206	n.m.	Galán et al. (2014)
Saanich Inlet, Canada	41	13–6720	40–633	n.m.	Michiels et al. (2019)
Western Indian Shelf	6	920–11650	n.d.-238	16–182	This study

(sulphide-free) shelf waters of Southwest India. This suggested that the chemolithoautotrophic denitrifiers have the potential to oxidize 100% of the sulphide accumulated in the water column or at least at the suboxic-anoxic interface as long as they are not limited by NO_x^- availability, which is evident from the fact that during early September, we often observe the shelf bottom water to be NO_x^--depleted but not sulphidic yet (Naqvi et al., 2006). This indicates a cryptic occurrence of sulphide-driven denitrification in the shelf bottom water precisely due to rapid oxidation of benthic-released sulphide by NO_2^- of the overlying suboxic water, creating an impression of NO_2^--depleted, non-sulphidic condition in the bottom water. A similar observation over the Namibian Shelf led Lavik et al. (2009) to postulate that many anoxic events in the coastal waters are probably not noticed due to faster and efficient oxidation of sulphide by NO_x^-, mediated by proliferating chemolithoautotrophs. This further suggested a possible co-occurrence of chemoorganotrophic denitrification in the NO_x^--rich suboxic intermediate layer and chemolithoautotrophic denitrification in the underlying anoxic bottom water (Fig. 9a). Consequently, it would create an optimal condition for the chemolithoautotrophic denitrification causing massive N loss over the WICS due to adequacy of substrates as NO_2^- is supplied through chemoorganotrophic denitrification in the overlying water and sulphide is supplied through SO_4^{2-} reduction in the underlying sediments. As the NO_x^- inventory is efficiently depleted through chemolithoautotrophic denitrification at the suboxic-anoxic interface, the thickness of suboxic layer wanes away progressively, and the sulphidic layer expands upward.

However, by early October, as the NO_x^--replete suboxic layer disappears completely and is replaced by NH_4^+-rich but NO_x^--depleted sulphidic layer; it leads to two layer stratification (i.e. oxic and anoxic) of the shelf water column (Naqvi et al., 2006). Although, the chemolithoautotrophic denitrification is expected to be limited by NO_x^- during this period, our measured high potential rate of this process in the sulphidic bottom water indicated the abundance and growth of chemolithoautotrophs which are possibly sustained by NO_x^- supply through nitrification. Having a high diffusive coefficient (Schulz et al., 2006), NH_4^+ in the sulphidic bottom water would be transported upwards by diffusion and turbulent mixing (Holtermann and Umlauf, 2012) and would get nitrified to NO_x^- at the oxic-anoxic interface, which in turn would be transported below the interface by the same processes to potentially support sulphide-driven denitrification (Fig. 9b). Such a coupling of nitrification and denitrification leading to higher N loss has been experimentally observed in the WICS waters (Krishnan et al., 2008) and elsewhere (Hietanen et al., 2012; Kalvelage et al., 2015). Although, the abundance of nitrifying bacteria in the anoxic shelf waters remains below detection (Krishnan et al., 2008), the possible proliferation of ammonium-oxidizing archaea (AOA) cannot be ruled out. Unlike ammonium-oxidizing bacteria (AOB) which cannot survive in sulphidic condition (Joye and Hollibaugh, 1995), AOA can thrive in sulphidic waters (Ergruder et al., 2009) with sulphide reaching up to 30 μM (Coolen et al., 2007). Thus, the sulphide-driven denitrification is possibly fed by archaeal nitrification in the NO_x^--depleted sulphidic shelf water as also observed by Hietanen et al. (2012) and Berg et al. (2015) in the Baltic Sea. Therefore, during October, the sulphide-driven denitrification is possibly sustained by being coupled to nitrification, and continues to cause N loss even in under NO_x^--limiting conditions.

4.6. *Impact of sulphide on N_2O cycling*

During our study, at the sulphidic stations, we frequently observed prominent N_2O peaks just at or above the oxic-anoxic interface, but very

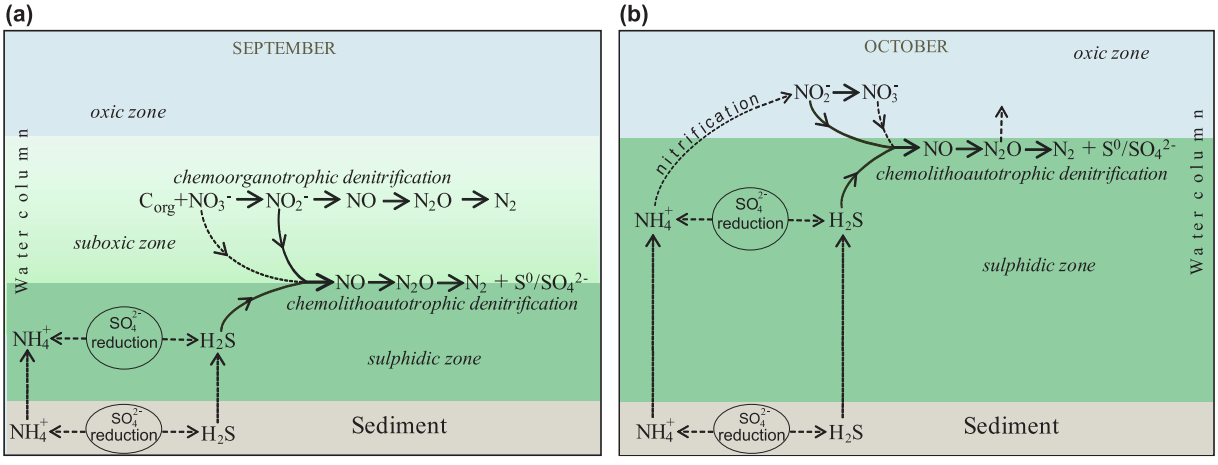

Fig. 9. A conceptual overview of the denitrification pathways in the WICS waters during (a) September and (b) October.

low N_2O in the sulphidic bottom water. A similar pattern of N_2O distribution is frequently observed during suboxia-anoxia transition phase over the WICS (Naqvi et al., 2006) and also in other sulphidic coastal systems (Brettar and Rheinheimer, 1991; Schunck et al., 2013). Such high and disproportionate N_2O build-up at the oxic-anoxic interface is therefore likely to be occurring due to (1) partial inhibition of N_2O reduction under microaerobic conditions (Naqvi et al., 2000; Dalsgaard et al., 2014; Arévalo-Martínez et al., 2015), (2) suppressed N_2O reductase enzyme (nosZ) activity is due to limitation of Cu (Granger and Ward, 2003; Sullivan et al., 2013) which precipitates with sulphide (Callbeck et al., 2021), and/or (3) N_2O production as a byproduct of ammonium oxidation occurring at low O_2 concentrations (Löscher et al., 2012; Xi et al., 2015). Our ^{15}N incubations showed much higher transient N_2O production with $^{15}NO_2^- + S^{2-}$ compared to $^{15}NO_2^-$ (Suppl. Figs. 3-10) at all the stations irrespective of them being suboxic or anoxic. After sulphide addition, concomitant with the higher N_2 production, transient N_2O accumulation increased by 1.4–44 fold at the suboxic stations and by 1.2–18 fold at the anoxic stations (Suppl. fig. 12). As the oxic-anoxic interface of the WICS water column is possibly subjected to frequent aeration (Naqvi et al., 2006), the further reduction of such high amounts of N_2O (to N_2) could be inhibited in situ, explaining its build-up at or just above the oxic-anoxic interface.

Contrastingly, non-detectable to undersaturated N_2O concentrations observed in the sulphidic bottom waters (Figs. 5, 6) was apparently due to its effective reduction to N_2 as evidenced in our $^{15}NO_2^- + S^{2-}$-amended incubations and bag incubations. Although, transient N_2O production was higher in the $^{15}NO_2^- + S^{2-}$ incubations than in the $^{15}NO_2^-$ incubations (Suppl. fig. 3–10, 12), there was no clear trend in the ratio of N_2 to N_2O production, and net N_2O consumption also began earlier in the $^{15}NO_2^- + S^{2-}$ incubations than in the $^{15}NO_2^-$ incubations. This indicated that the N_2O produced through sulphide-driven denitrification is more effectively reduced to N_2 than during chemoorganotrophic denitrification, supporting the evidence that sulphide-oxidizing denitrifiers have a high level of tolerance to sulphide (Jensen et al., 2009) and indicating that the chemolithoautotrophic denitrifiers in the WICS waters are capable of complete denitrification of NO_x^- to N_2 as reported in the Baltic Sea (Hietanen et al., 2012) and ETSP (Callbeck et al., 2018).

4.7. Chemoautotrophy and dark CO_2 fixation

Chemolithoauotrophic denitrifiers are known to fix CO_2 via reductive/reverse tricarboxylic acid (rTCA) cycle by using the energy gained from sulphide oxidation by NO_x^- (Campbell et al., 2006; Shao et al., 2010). Cultivated chemoautotrophic sulphide oxidizers have been observed to fix 0.22–0.37 mol of CO_2 per mole of NO_x^- reduced or 0.62 mol of H_2S oxidized (Callbeck et al., 2018 and references therein). Considering the mean autotrophic denitrification rate (2.69 μmol N_2 L^{-1} d^{-1}) and the N_2:NO_x^- ratio (Eq. 1), the mean NO_2^- consumption rate would be 0.22 μmol L^{-1} h^{-1} in the ^{15}N incubations, which is similar to the NO_2^- consumption rate observed in bag incubations i.e. 0.27 (±0.07) μmol L^{-1} h^{-1} (Section 3.4, Fig. 8). Considering the former rate, chemoautotrophic (dark) CO_2 fixation rate was conservatively estimated to be 1.18–1.98 μmol C L^{-1} d^{-1} which amounts to a mean depth-integrated rate of 0.21 (±0.07) g C m^{-2} d^{-1} assuming an 11 m-thick SMZ. The average primary productivity over the shelf during seasonal anoxia (September-October) i.e. 1.15 (±0.7) g C m^{-2} d^{-1} (Gauns et al., 2020) suggests that the chemoautotrophic (dark) C production was 18% of the photoautotrophic production and accounted for 15% of the total water column productivity. Jørgensen et al. (1991) observed dark CO_2 fixation rate occurring at the rate of 24–63 mg C m^{-2} d^{-1} and comprising 4–11% of the total primary production in the Black Sea. Taylor et al. (2001) reported that dark C fixation occurred at a rate of 0.32–1.9 g C m^{-2} d^{-1} which was 62% of the photoautotrophic C production in the Cariaco basin. Schunck et al. (2013) reported that the dark C fixation with a rate of 10.8–16.8 μg C L^{-1} d^{-1} accounted for 25% of the total CO_2 fixation over the Peruvian shelf. Thus, the dark CO_2 fixation rate and its contribution to total autotrophic C production over the WICS are comparable to those reported in the other anoxic coastal systems (Jørgensen et al., 1991; Taylor et al., 2001; Schunck et al., 2013) of the world.

4.8. Impact of chemolithoautotrophic denitrification on N, S and C budgets of the WICS

Over the WICS, sulphidic condition develops in the bottom water during early-mid September while the water column still has some amount of NO_x^-. By early October, the sulphidic condition spreads to a greater area of the shelf but the water column remains NO_x^--depleted. During late SW monsoon, 60,000 Km^2 areas of the WICS is considered to be functionally anoxic or denitrifying (Sarkar et al., 2020) which covers the innershelf and mid-shelf. However, by conservative estimates, the sulphidic zone occupies an area of 16,000 Km^2 of the innershelf, and the sulphidic bottom water underlain by or interspersed with NO_x^- -rich suboxic water persists at least for 1 month. Thus, considering the above factors, 11 m as the average thickness and 17.6×10^{10} m^3 as the volume of the SMZ, and mean N loss/transformation rates (Section 4.4), the N loss rate due to chemolithoautotrophic denitrification and anammox were 0.4 Tg N y^{-1} and 0.002 Tg N y^{-1}, respectively whereas N transformation rate due to DNRA was 0.004 Tg N y^{-1}. Previously, using NO_3^- consumption rate and assuming heterotrophic denitrification as the dominant N loss process, Naqvi et al. (2006) had estimated the N loss to be 1.3 Tg N y^{-1}. However, using ^{15}N incubations and considering the mean denitrification rate from a sulphidic year and two non-sulphidic (suboxic) years, Sarkar et al. (2020) reported the N loss rate to be 3.7 Tg N y^{-1}. The difference between the estimated annual N loss rates reported by the above authors and us arises apparently due to their consideration of denitrification occurring over a larger area (60,000 Km^2), broader depth range (20 m) and longer duration i.e. 90 days (August-October). Thus, considering the conservative estimate by Sarkar et al. (2020), the chemolithoautotrophic denitrification would account for ~ 11% of the total annual N loss in the shelf waters during seasonal anoxia. Additionally, chemolithoautotrophic denitrifiers potentially remove or oxidize 0.57 Tg of toxic sulphide from the shelf waters annually, taking the mean sulphide-driven denitrification rate and HS^-:N_2 ratio (Eq. 1) into account. This is probably the reason for the much lower sulphide accumulation in the anoxic WICS waters compared to other anoxic shallow marine systems of the world (Table 4). Upscaling of the estimated dark C fixation rate i.e. 0.21 g C m^{-2} d^{-1} over the anoxic shelf leads to an annual chemoautotrophic C fixation at the rate of 0.1 Tg C y^{-1}. Therefore, the prevalence of chemolithoautotrophic denitrification in the shelf waters can potentially impact the pelagic N, S and C budget of the WICS by removing significant quantity of extraneous N and toxic sulphide, and by adding extra C_{org}.

4.9. Implications for shelf biogeochemistry

Sulphide is toxic or lethal for many marine organisms (Petersen, 1977; Nicholls and Kim, 1982; Levin et al., 2009; Vaquer-Sunyer and Duarte, 2010), and as such, the abundance of many demersal fishes and benthic organisms are substantially reduced during sulphidic events on the WICS (Naqvi et al., 2006; Naqvi et al. 2009; Ingole et al., 2010). Our study implied that the sulphide-driven chemolithoautotrophic denitrification plays a crucial role in minimizing sulphide toxicity in the shelf waters. Although, sulphide is detected in the shelf bottom water around mid-September, NO_x^- is depleted in the same waters around a month earlier. It is highly likely that during this time the cryptic occurrence of sulphide-driven denitrification (supplied with NO_x^- diffusing from oxycline, see Fig. 9), is responsible for the removal of H_2S, and thereby it detoxifies the shelf bottom water during mid August to mid September. Even from mid to late September, sulphide level remains low which is apparently due to its effective oxidation via chemolithoautotrophic denitrification. Consequently, for about a month (mid August to mid

September), the shelf bottom water is effectively detoxified. Chemolithoautotrophic denitrification also seems to provide other crucial ecosystem services on the Western Indian Shelf as the sulphidic waters appear to be an effective sink for N_2O, partially ameliorating the massive accumulations of this potent greenhouse gas that occur at the pelagic oxycline. Efficient carbon retention through dark CO_2 fixation possibly sustains the intensity and the duration of euxinic regime over the shelf. Thus, by causing rapid N loss, sulphide oxidation and significant dark CO_2 fixation, chemolithoautotrophic denitrification reduces N_2O and CO_2 emission, retains carbon in the shelf system and links three key elements i.e. C, N and S of the shelf biogeochemical cycle. With the increasing expansion and intensification of OMZs, increase in the number of dead zones, and increasing frequency of sulphidic events, chemolithoautotrophic denitrification is expected to play a greater role in N cycling and budgets of shallow marine systems in future.

CRediT authorship contribution statement

Anil Pratihary: Conceptualization, Methodology, Formal analysis, Investigation, Writing – original draft. **Gaute Lavik:** Formal analysis, Writing – review & editing. **S.W.A. Naqvi:** Supervision, Methodology, Investigation, Project administration. **Gayatri Shirodkar:** Investigation. **Amit Sarkar:** Investigation. **Hannah Marchant:** Writing – review & editing. **Thomas Ohde:** Investigation. **Damodar Shenoy:** Investigation, Funding acquisition. **Siby Kurian:** Investigation, Funding acquisition. **Hema Uskaikar:** Investigation, Funding acquisition. **Marcel M.M. Kuypers:** Supervision, Funding acquisition.

Declaration of Competing Interest

The authors declare that they have no known competing financial interests or personal relationships that could have appeared to influence the work reported in this paper.

Data availability

The data that has been used is confidential.

Acknowledgements

The authors wish to thank the Directors of CSIR-National Institute of Oceanography (NIO) and Max Planck Institute for Marine Microbiology (MPIMM) for providing logistics and laboratory facilities for this work which was carried out as AP's post-doctoral research that formed a part of collaborative programme between NIO and MPIMM. AP gratefully acknowledges DAAD (German Academic Exchange Service) for the Post-doctoral Fellowship and funding this research programme. SWAN acknowledges the European Commission for the Marie Curie International Incoming Fellowship. AS and GS duly acknowledge CSIR for the Senior Research Fellowships. HKM was funded by the DFG Cluster of Excellence "The Ocean Floor – Earth's Uncharted Interface" at MARUM, University of Bremen (EXC-2077). We also thank Gabi Klockgether, Goudong Song and Jessika Füssel for their kind help in the analyses at MPIMM. Ankita Chari and Sushma Naik are duly acknowledged for their assistance in nutrients and N_2O analysis, respectively. The MERIS data were kindly provided by ESA. We thankfully acknowledge the use of MODIS data from LANCE FIRMS operated by the NASA/GSFC/Earth Science Data and Information System (ESDIS) with funding provided by NASA/HQ. We thank Dr. I. Suresh and Dr. Mangesh Gauns for the valuable discussions. The captain and crew of *R/V Sindhu Sankalp* (SSK-24) are duly acknowledged for their kind help and logistic support. We thank the Editor for considering the manuscript for the review and publication, and the anonymous reviewers for their thorough and critical reviews which greatly improved the quality of the paper. This research work was also partly funded by CSIR through NIO's network project PSC0108, and by MoES through the SIBER-India projects GAP2424 and GAP2425. This is CSIR-NIO's contribution no. 7089.

Appendix A. Supplementary data

Supplementary data to this article can be found online at https://doi.org/10.1016/j.pocean.2023.103075.

References

Arévalo-Martínez, D.L., Kock, A., Löscher, C.R., Schmitz, R.A., Bange, H.W., 2015. Massive nitrous oxide emissions from the tropical South Pacific Ocean. Nat. Geosci. 8, 530–535.

Arévalo-Martínez, D.L., Steinhoff, T., Brandt, P., Körtinger, A., Lamont, T., Rehder, G., Bange, H.W., 2019. N2O emissions from the northern Benguela upwelling system. Geophys. Res. Lett. 46, 3317–3326.

Bardhan, P., Naqvi, S.W.A., 2020. Nitrogen and carbon cycling over the western continental shelf of India during seasonal anoxia: A stable isotope approach. J. Mar. Syst. 207, 103144.

Berg, C., Vandieken, V., Thamdrup, B., Jürgens, K., 2015. Significance of archaeal nitrification in hypoxic waters of the Baltic Sea. ISME J. 9, 1319–1332.

Bernard, R.J., Mortazavi, B., Kleinhuizan, A.A., 2015. Dissimilatory nitrate reduction to ammonium (DNRA) seasonally dominates NO_3^- reduction pathways in an anthropogenically impacted sub-tropical coastal lagoon. Biogeochemistry 125, 47–64.

Bonaglia, S., Klawonn, I., Brabandere, L.D., Deutsch, B., Thamdrup, B., Brüchert, V., 2016. Denitrification and DNRA at the Baltic Sea oxic-anoxic interface: Substrate spectrum and kinetics. Limnol. Oceanogr. 61, 1900–1915.

Breitburg, D., Levin, L.A., Oschlies, A., Grégoire, M., Chavez, F.P., Conley, D.J., Garçon, V., Gilbert, D., Gutierrez, D., Isensee, K., Jacinto, G.S., Limberg, K.E., Montes, I., Naqvi, S.W.A., Pitcher, G.C., Rabalais, N.N., Roman, M.R., Rose, K.A., Seibel, B.A., Telszewski, M., Yasuhara, M., Zhang, J., 2018. Declining oxygen in the global ocean and coastal waters. Science 359, eaam7240. https://doi.org/10.1126/science.aam7240.

Brettar, I., Rheinheimer, G., 1991. Denitrification in the Central Baltic Sea: evidence for H_2S-oxidation as motor of denitrification at the oxic-anoxic interface. Mar. Ecol. Prog. Ser. 77, 157–169.

Brettar, I., Labrenz, M., Flavier, S., Bötel, J., Kuosa, H., Christen, R., Höfle, M.G., 2006. Identification of a Thiomicrospira denitrificans-Like Epsilonproteobacterium as a catalyst for autotrophic denitrification in the Central Baltic Sea. Appl. Eniron. Microbiol. 72 (2), 1364–1372.

Bristow, L.A., Dalsgaard, T., Tiano, L., Mills, D.B., Bertagnolli, A.D., Wright, J.J., Hallam, S.J., Ulloa, O., Canfield, D.E., Revsbech, N.P., Thamdrup, B., 2016. Ammonium and nitrite oxidation at nanomolar oxygen concentrations in oxygen minimum zone waters. PNAS 113 (38), 10601–10606.

Burgin, A.J., Hamilton, S.K., 2008. NO3–driven SO42- production in freshwater ecosystems: Implications for N and S cycling. Ecosystems 11, 908–922.

Callbeck, C.M., Canfield, D.E., Kuypers, M.M.M., Yilmaz, P., Lavik, G., Thamdrup, B., Schubert, C.J., Bristow, L.A., 2021. Sulfur cycling in oceanic oxygen minimum zones. Limnol. Oceanogr. 9999, 1–33.

Callbeck, C.M., Lavik, G., Ferdelman, T.G., Fuchs, B., Gruber-Vodicka, H.R., Hach, P.F., Littman, S., Schoffelen, N.J., Kalvelage, T., Thomsen, S., Schunck, H., Loscher, C.R., Schmitz, R.A., 2018. Oxygen minimum zone cryptic sulphur cycling sustained by offshore transport of key sulphur oxidizing bacteria. Nat. Commun. 9, 1–11.

Campbell, B.J., Engel, A.S., Porter, M.L., Takai, K., 2006. The versatile ε-proteobacteria: key players in sulphidic habitats. Nat. Rev. Microbiol. 4, 458–468.

Canfield, D.E., Stewart, F.J., Thamdrup, B., De Brabandere, L., Dalsgaard, T., Delong, E. F., Revsbech, N.P., Ulloa, O., 2010. A cryptic sulphur cycle in the oxygen-minimum-zone waters off the Chilean coast. Science 330, 1375–1378.

Codispoti, L.A., Brandes, J.A., Christensen, J.P., Devol, A.H., Naqvi, S.W.A., Paerl, H.W., Yoshinari, T., 2001. The oceanic fixed nitrogen and nitrous oxide budgets: Moving targets as we enter the anthropocene? Sci. Mar. 65, 85–105.

Coolen, M.J.L., Abbas, B., Van Bleijswijk, J., Hopmans, E.C., Kuypers, M.M.M., Wakeham, S.G., 2007. Putative ammonia-oxidizing Crenarchaeota in suboxic waters of the Black Sea: a basin-wide ecological study using 16S ribosomal and functional genes and membrane lipids. Environ. Microbiol. 9, 1001–1016.

Dalsgaard, T., Canfield, D.E., Petersen, J., Thamdrup, B., Acuña-González, J., 2003. N_2 production by the anammox reaction in the anoxic water column of Golfo Dulce, Costa Rica. Nature 422, 606–608.

Dalsgaard, T., Brabandere, L.D., Hall, P.O.J., 2013. Denitrification in the water column of the central Baltic Sea. Geochim. Cosmochim. Acta 106, 247–260.

Dalsgaard, T., Stewart, F.J., Thamdrup, B., De Brabandere, L., Revsbech, N.P., Ulloa, O., Canfield, D.E., DeLong, E.F., 2014. Oxygen at nanomolar levels reversibly suppresses process rates and gene expression in anammox and denitrification in the oxygen minimum zone off Northern Chile. Am. Soc. Microbiol. 5 (6), e01966–e2014.

Dalsgaard, T., Thamdrup, B., Farias, L., Revsbech, N.P., 2012. Anammox and denitrification in the oxygen minimum zone of the eastern South Pacific. Limnol. Oceangr. 57 (5), 1331–1346.

De Brabandere, L., Canfield, D.E., Dalsgaard, T., Friederich, G.E., Revsbech, N.P., Ulloa, O., Thamdrup, B., 2014. Vertical partitioning of nitrogen-loss processes across the oxic-anoxic interface of an oceanic oxygen minimum zone. Environ. Microbiol. 16 (10), 3041–3054.

Diaz, R.J., Rosenberg, R., 2008. Spreading dead zones and consequences for marine ecosystems. Science 321, 926–929.

Ergruder, T.H., Boon, N., Wittebolle, L., Marzorati, M., Verstraete, W., 2009. Environmental factors shaping the ecological niches of ammonia-oxidizing archaea. FEMS Microbiol. Rev. 33, 855–869.

Falkowski, P.G., Evolution of the nitrogen cycle and its influence on the biological sequestration of CO_2 in the ocean. Nature 387, 272-275.

Fuchsman, C.A., Murray, J.W., Staley, J.T., 2012. Stimulation of autotrophic denitrification by intrusions of the Bosporus Plume into the anoxic Black Sea. Front. Microbiol. 3, 1–14.

Füssel, J., Lam, P., Lavik, G., Jensen, M.M., Holtappels, M., Günter, M., Kuypers, M.M.M., 2012. Nitrite oxidation in the Namibian oxygen minimum zone. The ISME J. 6, 1200–1209.

Galán, A., Faúndez, J., Thamdrup, B., Santibáñez, J.F., Farías, L., 2014. Temporal dynamics of nitrogen loss in the coastal upwelling ecosystem off central Chile: Evidence of autotrophic denitrification through sulfide oxidation. Limnol. Oceanogr. 59 (6), 1865–1878.

Gauns, M., Mochemadkar, S., Pratihary, A., Shirodkar, G., Narvekar, P.V., Naqvi, S.W.A., 2020. Phytoplankton associated with seasonal oxygen depletion in waters of the western continental shelf of India. J. Mar. Syst. 204, 103308.

Gilbert, D., Rabalais, N.N., Díaz, R.J., Zhang, J., 2010. Evidence for greater oxygen decline rates in the coastal ocean than in the open ocean. Biogeosciences 7, 2283–2296.

Glaubitz, S., Leuders, T., Abraham, W.R., Jost, G., Jurgens, K., Labrenz, M., 2009. 13C-isotope analyses reveal that chemolithoautotrophic Gamma- and Epsilonproteobacteria feed microbial food web in a pelagic redoxclines of the Central Baltic Sea. Environ. Microbiol. 11 (2), 326–337.

Glaubitz, S., Labrenz, M., Jost, G., Jürgens, K., 2010. Diversity of active chemolithoautotrophic prokaryotes in the sulfidic zone of a Black Sea pelagic redoxclines as determined by rRNA-based stable isotope probing. FEMS Microbiol. Ecol. 74, 32–41.

Glaubitz, S., Kießlich, K., Meeske, C., Labrenz, M., Jürgens, K., 2013. SUP05 dominates the Gammaproteobacterial sulfur oxidizer assemblages in pelagic redoxclines of the Central Baltic and Black Sea. Appl. Environ. Microbiol. 79 (8), 2767–2776.

Gomes, J., Khandeparker, R., Bandekar, M., Meena, R.M., Ramaiah, N., 2018. Quantitative analyses of denitrifying bacterial diversity from a seasonally hypoxic monsoon governed tropical coastal region. Deep Sea Res. II, 34–43.

Gomes, J., Khandeparker, R., Naik, H., Shenoy, D., Meena, R.M., Ramaiah, N., 2020. Denitrification rates of culturable bacteria from a coastal location turning temporally hypoxic. J. Mar. Syst. 209, 103089.

Granger, J., Ward, B.B., 2003. Accumulation of nitrogen oxides in copper-limited cultures of denitrifying bacteria. Limnol. Oceanogr., 48(1), 313-318.

Grasshoff, K., Kremling, K., Ehrhardt, M., 1999. Methods of Seawater Analysis, 3rd ed. Wiley-VCH Verlag GmbH.

Grote, J., Schott, T., Bruckner, C.G., Glöckner, F.O., Jost, G., Teeling, H., Labrenz, M., Jürgens, K., 2012. Genome and physiology of a model Epsilonproteobacterium responsible for sulfide detoxification in marine oxygen depletion zones. Proc. Natl. Acad. Sci. 109, 506–510.

Gruber N., Sarmiento, J. L., 2002. Large-scale biogeochemical-physical interactions in elemental cycles. P. 337-399. In: A.R. Robinson, J.J. McCarthy and B.J. Rothschild [eds], The Sea, Vol. 12, John Wiley and Sons.

Gupta, G.V.M., Sudheesh, V., Sudharma, K.V., Saravanane, N., Dhanya, V., Dhanya, K.R., Lakshmi, G., Sudhakar, M., Naqvi, S.W.A., 2016. Evolution to decay of upwelling and associated biogeochemistry over the southeastern Arabian Sea shelf. J. Geophys. Res.: Biogeosci. 121, 159–175.

Gupta, G.V.M., Jyothibabu, R., Ramu, C.V., Reddy, A.Y., Balachandran, K.K., Sudheesh, V., Kumar, S., Chari, N.V.H.K., Bepari, K.F., Marathe, P.H., Reddy, B.B., Vijayan, A.K., 2021. The world's largest coastal deoxygenation zone is not anthropogenically driven. Environ. Res. Lett. 16, 054009.

Hamersley, M.R., Lavik, G., Woebken, D., Rattray, J.E., Lam, P., Hopmans, E.C., Sinninghe Damsté, Krüger, S., Graco, M., Gutiérrez, D., Kuypers, M.M.M., 2007. Anaerobic ammonium oxidation in the Peruvian oxygen minimum zone. Limnol. Oceangr. 52 (3), 923–933.

Hannig, M., Lavik, G., Kuypers, M.M.M., Woebken, D., Martens-Habbena, W., Jürgens, K., 2007. Shift from denitrification to anammox after inflow events in the central Baltic Sea. Limnol. Oceanogr. 52 (4), 1336–1345.

Hietanen, S., Jantti, H., Buizert, C., Jürgens, K., Labrenz, M., Voss, M., Kuparinen, J., 2012. Hypoxia and nitrogen processing in the Baltic Sea water column. Limnol. Oceanogr. 57 (1), 325–337.

Holtappels, M., Lavik, G., Jensen, M.M., Kuypers, M.M.M., 2011. ^{15}N-Labelling experiments to dissect the contributions of heterotrophic denitrification and anammox to nitrogen removal in the OMZ waters of the ocean. Methods Enzymol. 486, 223–251.

Holtermann, P.L., Umlauf, L., 2012. The Baltic Sea tracer release experiment: 2. Mixing processes. J. Geophys. Res. 117 (C01022), 2012. https://doi.org/10.1029/2011JC007445.

Hügler, M., Wirsen, C.O., Fuchs, G., Taylor, C.D., Sievert, S.M., 2005. Evidence for autotrophic CO_2 fixation via the reductive tricarboxylic acid cycle by members of the ε subdivision of proteobacteria. J. Bacteriol. 187 (9), 3020–3027.

Ingole, B.S., Sautya, S., Sivadas, S., Singh, R., Nanajkar, M., 2010. Macrofaunal community structure in the western Indian continental margin including the oxygen minimum zone. Mar. Ecol. Evol. Persp. 31, 148–166.

Jayakumar, D.A., Francis, C.A., Naqvi, S.W.A., Ward, B.B., 2004. Diversity of nitrite reductase genes (*nirS*) in the denitrifying water column of the coastal Arabian Sea. Aquat. Microb. Ecol. 34, 69–78.

Jensen, M.M., Kuypers, M.M.M., Lavik, G., Thamdrup, B., 2008. Rates and regulation of anaerobic ammonium oxidation and denitrification in the Black Sea. Limnol. Oceanogr. 53 (1), 23–36.

Jensen, M.M., Lam, P., Revsbech, N.P., Nagel, B., Gaye, B., Jetten, M.S.M., Kuypers, M.M.M., 2011. Intensive nitrogen loss over the Omani shelf due to anammox coupled with dissimilatory nitrite reduction to ammonium. ISME J. 5, 1660–1670.

Jensen, M.M., Petersen, J., Dalsgaard, T., Thamdrup, B., 2009. Pathways, rates, and regulation of N_2production in the chemocline of an anoxic basin, Mariager Fjord. Denmark. Mar. Chem. 113, 102–113.

Jørgensen, B.B., Fossing, H., Wirsen, C.O., Jannasch, H.W., 1991. Sulfide oxidation in the anoxic Black Sea chemocline. Deep-Sea Res. 38, S1083–S1103.

Jost, G., Zubkov, M.V., Yakushev, E., Labrenz, M., Jürgens, K., 2008. High abundance and dark CO2 fixation of chemolithoautotrophic prokaryotes in anoxic waters of the Baltic Sea. Limnol. Oceanogr. 53 (1), 14–22.

Joye, S., Hollibaugh, J.T., 1995. Influence of sulfide inhibition of nitrification on nitrogen regeneration in sediments. Science 270, 623–625.

Kalvelage, T., Lavik, G., Jensen, M.M., Revsbech, N.P., Löscher, C., Schunck, H., Desai, D. K., Hauss, H., Kiko, R., Holtappels, M., LaRoache, J., Schmitz, R.A., Graco, M.I., Kuypers, M.M., 2015. Aerobic microbial respiration in oceanic oxygen minimum zones. PLoS One 10 (7), e0133526.

Kamaleson, A.S., Gaosalves, M.J., Kumar, S., Jineesh, V.K., Lokabharathi, P.A., 2019. Spatio-temporal variations in sulfur-oxidizing and sulfate-reducing bacterial activities during upwelling, off south-west coast of India. Oceanologia 61, 427–444.

Kartal, B., Kuypers, M.M.M., Lavik, G., Schalk, J., Op den Camp, H.J.M., Jetten, M.S.M., Strous, M., 2007. Anammox bacteria disguised as denitrifiers: nitrate reduction to dinitrogen gas via nitrite and ammonium. Environ. Microbiol. 9 (3), 635–642.

Krishnan, K.P., Fernandes, S.O., Loka Bharathi, P.A., Krishna Kumari, L., Nair, S., Pratihary, A.K., Rao, B.R., 2008. Anoxia over the western continental shelf of India: Bacterial indications of intrinsic nitrification feeding denitrification. Mar. Environ. Res. 65, 445–455.

Kuypers, M.M.M., Sliekers, A.O., Lavik, G., Schmid, M., Jørgensen, B.B., Kuenen, J.G., Damste, J.S.S., Strous, M., Jetten, M.S.M., 2003. Anaerobic ammonium oxidation by anammox bacteria in the Black Sea. Nature 422, 608–611.

Kuypers, M.M.M., Lavik, G., Woebken, D., Schmid, M., Fuchs, B.M., Amann, R., Jørgensen, B.B., Jetten, M.S.M., 2005. Massive nitrogen loss from the Benguela upwelling system through anaerobic ammonium oxidation. Proc. Natl. Acad. Sci. 102, 6478–6483.

Lam, P., Kuypers, M.M.M., 2011. Microbial nitrogen cycling processes in oxygen minimum zones. Annu. Rev. Mar. Sci. 3, 317–345.

Lam, P., Lavik, G., Jensen, M.M., van de Vossenberg, J., Schmid, M., Woebken, D., Gutiérrez, D., Amann, R., Jetten, M.S.M., Kuypers, M.M.M., 2009. Rivising the nitrogen cycle in the Peruvian oxygen minimum zone. PNAS 106 (12), 4752–4757.

Lavik, G., Stuhrmann, T., Brüchert, V., Van der Plas, A., Mohrholz, V., Lam, P., Musmann, M., Fuchs, B.M., Amann, R., Lass, U., Kuypers, M.M.M., 2009. Detoxification of sulphidic African shelf waters by blooming chemolithotrophs. Nature 457, 581–585.

Levin, L.A., Ekau, W., Gooday, A.J., Jorissen, F., Middelburg, J.J., Naqvi, S.W.A., Neira, C., Rabalais, N.N., Zhang, J., 2009. Effects of natural and human-induced hypoxia on coastal benthos. Biogeosciences 6, 2063–2098.

Löscher, C.R., Kock, A., Könneke, M., LaRoche, J., Bange, H.W., Schmitz, R.A., 2012. Production of oceanic nitrous oxide by ammonia-oxidizing archaea. Biogeosciences 9, 2419–2429.

Mallik, T.K., 2008. Marine Geology: A scenario around Indian coasts. New Academic Publishers.

Manning, C.C., Hamme, R.C., Bourbonnais, A., 2010. Impact of deep-water renewal events on fixed nitrogen loss from seasonally-anoxic Saanich inlet. Mar. Chem. 122, 1–10.

Marchant, H.K., Tegetmeyer, H.E., Ahmerkamp, S., Holtappels, M., Lavik, G., Graf, J., Schreiber, F., Mussman, M., Strous, M., Kuypers, M.M.M., 2018. Metabolic specialization of denitrifiers in permeable sediments controls N_2O emissions. Environ. Microbiol. 20 (12), 4486–4502.

McAuliffe, C., 1971. GC determination of solutes by multiple phase equilibration. Chem. Technol. 1, 46–50.

Michiels, C.C., Huggins, J.A., Giesbrecht, K.E., Spence, J.S., Simister, R.L., Varela, D.E., Hallam, S.J., Crowe, S.A., 2019. Rates and pathways of N2 production in a persistently anoxic fjord: Saanich Inlet. British Columbia. Front. Mar. Sci. 6, 27. https://doi.org/10.3389/fmars.2019.00027.

Millero, F.J., 1986. The thermodynamics and kinetics of the hydrogen sulphide system in natural waters. Mar. Chem. 81, 121–147.

Montes, E., Altabet, M.A., Muller-Karger, F.E., Scranton, M.I., Thunell, R.C., Benitez-Nelson, C., Lorenzoni, L., Astor, Y.M., 2013. Biogenic nitrogen gas production at the oxic-anoxic interface in the Cariaco basin, Venezuela. Biogeosciences 10, 267–279.

Naik, V., Damare, S.R., Shah, S.S., Shenoy, D.M., Mulla, A.B., in preparation. Coastal hypoxia drives microbial diversity: Elucidation through 16S rRNA amplicon sequencing.

Naqvi, S.W.A., Noronha, R.J., 1991. Nitrous oxide in the Arabian Sea. Deep-Sea Res. 38 (7), 871-890.

Naqvi, S. W. A., H. Naik, D. A. Jayakumar, M. S. Shailaja, and P. V. Narvekar. 2006. Seasonal oxygen deficiency over the western continental shelf of India, p. 195–224. In L. N. Neretin [ed.], Past and Present Water Column Anoxia. Springer.

Naqvi, S.W.A., Naik, H., Jayakumar, A., Pratihary, A.K., Narvekar, G., Kurian S., Agnihotri, R., Shailaja, M.S., Narvekar, P.V., 2009. Seasonal anoxia over the Western Indian continental shelf. In: Wiggert, J.D., Hood, R.R., Naqvi, S.W.A., Brink, K.H., Smith, S.L. (Eds.), Indian Ocean biogeochemical processes and ecological variability, Geophysical Monograph Series, Vol. 185, Americal Geophysical Union, pp. 333-345.

Naqvi, S.W.A., Jayakumar, D.A., Narvekar, P.V., Naik, H., Sarma, V.V.S.S., D'Souza, W., Joseph, S., George, M.D., 2000. Increased marine production of N_2O due to intensifying anoxia on the Indian continental shelf. Nature 408, 346–349.

Naqvi, S.W.A., Bange, H.W., Farias, L., Monteiro, P.M.S., Scranton, M.I., Zhang, J., 2010. Marine hypoxia/anoxia as a source of CH_4 and N_2O. Biogeosciences 7, 2159–2190.
Nicholls, P., Kim, J.K., 1982. Sulfide as an inhibitor and electron donor for the cytochrome-c oxidase system. Can. J. Biochem. Cell B 60, 613–623.
Ohde, T., 2018. Coastal sulfur plumes off Peru during El Nino, La Nina, and neutral phases. Geophys. Res. Lett. 45 https://doi.org/10.1029/2018GL077618.
Ohde, T., Dadou, I., 2018. Seasonal and annual variability of coastal sulphur plumes in the northern Benguela upwelling system. PLoS One 13 (2), e0192140. https://doi.org/10.1371/journal.pone.0192140.
Parvathi, V., Suresh, I., Langaigne, M., Ethe, C., Vialard, J., Levy, M., Neetu, S., Aumont, O., Resplandy, L., Naik, H., Naqvi, W., 2017. Positive Indian Ocean Dipole events prevents anoxia off the west coast of India. Biogeosciences 14, 1541–1559.
Petersen, L.C., 1977. Effect of inhibitors on oxygen kinetics of cytochrome-c oxidase. Biochim. Biophys. Acta 460, 299–307.
Pitcher, G.C., Aguirre-Velarde, A., Breitburg, D., Cardich, J., Carstensen, J., Conley, D.J., Dewitte, B., Engel, A., Espinoza-Morriberón, D., Flores, G., Garçon, V., Graco, M., Grégoire, M., Gutiérrez, D., Hernandez-Ayon, J.M., Huang, H.M., Isensee, K., Jacinto, M.E., Levin, L., Lorenzo, A., Machu, E., Merma, L., Montes, I., Naqvi, S.W.A., Paulmier, A., Roman, M., Rose, K., Hood, R., Rabalais, N.N., Salvanes, A.G., Salvatecci, R., Sànchez, S., Sifeddine, A., Tall, A.W., van der Plas, A.K., Yasuhara, M., Zhang, J., Zhu, Z., 2021. System controls of coastal and open ocean oxygen depletion. Prog. Oceangr. 197, 102613.
Pratihary, A.K., Naqvi, S.W.A., Narvenkar, G., Kurian, S., Naik, H., Naik, R., Manjuanatha, B.R., 2014. Benthic mineralization and nutrient exchange over the inner continental shelf of western India. Biogeosciences 11, 2771–2791.
Pratihary, A., Shenoy, D.M., Gauns, M., Mochemadkar, S., Araujo, J., Morajkar, S., Bepari, K., Ahmed, A., in preparation. Benthic-pelagic coupling over the Eastern Arabian Sea Shelf.
Preisler, A., de Beer, D., Lichtschlag, A., Lavik, G., Boetius, A., Jørgensen, B.B., 2007. Biological and chemical oxidation in a Beggiatoa inhabited marine sediment. ISME J. 1, 341–353.
Rao, A.D., Joshi, M., Ravichandran, M., 2008. Oceanic upwelling and downwelling processes in waters off the west coast of India. Ocean Dyn. 58, 213–226.
Sarkar, A., Naqvi, S.W.A., Lavik, G., Pratihary, A., Naik, H., Shirodkar, G., Kuypers, M.M.M., 2020. Massive nitrogen loss over the western Indian continental shelf during seasonal anoxia: Evidence from isotope pairing technique. Front. Mar. Sci. 7, 1–14.
Schulz, H.D., 2006. Quantification of early diagenesis: Dissolved constituents in pore water and signals in the solid phase. In: Schulz, H.D., Zabel, M. (Eds.), Marine Geochemistry. Springer, pp. 73–124.
Schunck, H., Lavik, G., Deasi, D.K., Großkopf, T., Kalvelage, T., Loscher, C.R., Paulmier, A., Contreras, S., Siegel, H., Holtappels, M., Rosenstiel, P., Schilhabel, M. B., Graco, M., Schmitz, R.A., Kuypers, M.M.M., LaRoache, J., 2013. Giant hydrogen sulphide plume in the oxygen minimum zone off Peru supports chemolithoautotrophy. PLoS One 8, 1–18.
Shao, M.F., Zhang, T., Fang, H.P., 2010. Sulfur-driven autotrophic denitrification: diversity, biochemistry, and engineering applications. Appl. Microbiol. Biotechnol. 88, 1027–1042.
Shenoi, S., Antony, M.K., 1991. Current measurements over the western continental shelf of India. Cont. Shelf Res. 11 (1), 81–93.
Shirodkar, G., Naqvi, S.W.A., Naik, H., Pratihry, A.K., Kurian, S., Shenoy, D.M., 2018. Methane dynamics in the shelf waters of the West coast of India during seasonal anoxia. Mar. Chem. 203, 55–63.
Song, G.D., Liu, S.M., Kuypers, M.M.M., Lavik, G., 2016. Application of the isotope pairing technique in sediments where anammox, denitrification and dissimilatory nitrate reduction to ammonium coexist. Limnol. Oceanogr.: Methods 14, 801–815.
Stramma, L., Johnson, G.C., Sprintall, J., Mohrholz, V., 2008. Expanding oxygen minimum zones in the tropical oceans. Science 320, 655–658.
Sullivan, M.J., Gates, A.J., Appia-Ayme, C., Rowley, G., Richardson, D.J., 2013. Copper control of bacterial nitrous oxide emission and its impact on vitamin B12-dependent metabolism. PNAS 110, 19926–19931.
Suter, E.A., Pachiadaki, M.G., Montes, E., Edgcomb, V.P., Scranton, M.I., Taylor, C.D., Taylor, G.T., 2021. Diverse nitrogen cycling pathways across a marine oxygen gradient indicate nitrogen loss coupled to chemoautotrophic activity. Environ. Microbiol. 23 (6), 2747–2764.
Taylor, G.T., Iabichella, M., Ho, T.Y., Scranton, M.I., Thunell, R.C., Muller-Karger, F., Varela, R., 2001. Chemoautotrophy in the redox transition zone of the Cariaco Basin: A significant midwater source of organic carbon production. Limnol. Oceangr. 46 (1), 148–163.
Thamdrup, B., Dalsgaard, T., Jensen, M.M., Ulloa, O., Farias, L., Escribano, R., 2006. Anaerobic ammonium oxidation in the oxygen-deficient waters off northern Chile. Limnol. Oceanogr. 51 (5), 2145–2156.
Tyrrell, T., 1999. The relative influences of nitrogen and phosphorus on oceanic primary production. Nature 400, 525–531.
Unnikrishnan, A.S., Antony, M.K., 1990. On the vertical velocity fluctuations and internal tides in an upwelling region of the West coast of India. Estuar. Coast. Shelf Sci. 31, 865–873.
Van Vliet, D.M., von Meijenfeldt, F.A.B., Dutilh, B.E., Sinninge-Damsté, J.S., Stams, J.M., Sánchez-Andrea, I., 2020. The bacterial sulfur cycle in expanding dysoxic and euxinic marine waters. Eniron. Microbiol. 23 (6), 2834–2857.
Vaquer-Sunyer, R., Duarte, C.M., 2010. Sulfide exposure accelerates hypoxia-driven mortality. Limnol. Oceanogr. 55 (3), 1075–1082.
Walsh, D.A., Zaikova, E., Howes, C.G., Song, Y.C., Wright, J.J., Tringe, S.G., Tortell, P.D., Hallam, S.J., 2009. Metagenome of a versatile chemolithoautotroph from expanding oceanic dead zones. Science 326, 578–582.
Ward, B.B., Tuit, C.B., Jayakumar, A., Rich, J.J., Moffett, J., Naqvi, S.W.A., 2008. Organic carbon, and not copper, controls denitrification in oxygen minimum zones of the ocean. Deep-Sea Res. I 55, 1672–1683.
Warembourg, F.R., 1993. Nitrogen fixation in soil and plant systems. In: Knowles, R., Paul, E.A., Melillo, J., Blackburn, H. (Eds.), Nitrogen Isotope Techniques. Academic Press, pp. 127–156.
Xi, Q., Babbin, A., Jayakumar, A., Oleynik, S., Ward, B.B., 2015. Nitrous oxide production by nitrification and denitrification in the Eastern Tropical South Pacific oxygen minimum zone. Geophys. Res. Lett. 42, 10755–10764. https://doi.org/10.1002/2015GL066853.